



## Scales and causes of heterogeneity in bars in a large multi-channel river: Río Paraná, Argentina

Journal:	<i>Sedimentology</i>
Manuscript ID:	SED-2013-OM-018.R1
Manuscript Type:	Original Manuscript
Date Submitted by the Author:	28-Aug-2013
Complete List of Authors:	Reesink, Arnold Jan Herman; University of Hull, Department of Geography, Environment and Earth Sciences Ashworth, Phil; Brighton university, Geography Division sambrook smith, gregory; University of Birmingham, School of Geography Best, Jim; University of Illinois, Geology Parsons, Daniel; University of Hull, Geography, Environment and Earth Sciences Amsler, Mario; Universidad Nacional del Litoral, Facultad de Ingeniería y Ciencias Hídricas Hardy, Richard; Durham University, Geography; Lane, Stuart; University of Lausanne, Institut de géographie Nicholas, Andrew; University of Exeter, School of Geography Orfeo, Oscar; CECOAL - CONICET, Sedimentology; Sandbach, Steven; University of Exeter, Department of Geography Simpson, Christopher; Fulcrum Graphic Communications Inc., Szupiany, Ricardo; Universidad Nacional del Litoral, Facultad de Ingeniería y Ciencias Hídricas
Keywords:	Large rivers, Bars, Río Paraná, Facies models, Channel deposits, GPR, Dunes

SCHOLARONE™  
Manuscripts

This is the peer reviewed version of the following article: Reesink, A. J. H., Ashworth, P. J., Sambrook Smith, G. H., Best, J. L., Parsons, D. R., Amsler, M. L., Hardy, R. J., Lane, S. N., Nicholas, A. P., Orfeo, O., Sandbach, S. D., Simpson, C. J. and Szupiany, R. N. (2014), Scales and causes of heterogeneity in bars in a large multi-channel river: Río Paraná, Argentina. *Sedimentology*, 61: 1055–1085. doi:10.1111/sed.12092, which has been published in final form at <http://onlinelibrary.wiley.com/doi/10.1111/sed.12092/abstract>. This article may be used for non-commercial purposes in accordance with Wiley Terms and Conditions for Self-Archiving.

1  
2 **Scales and causes of heterogeneity in bars in a large multi-channel river:**  
3  
4 **Río Paraná, Argentina**  
5  
6  
7  
8

9  
10 ARNOLD J.H. REESINK<sup>1,2\*</sup>, PHILIP J. ASHWORTH<sup>1</sup>, GREGORY H. SAMBROOK SMITH<sup>2</sup>,  
11 JAMES L. BEST<sup>3</sup>, DANIEL R. PARSONS<sup>4</sup>, MARIO L. AMSLER<sup>5</sup>, RICHARD J. HARDY<sup>6</sup>,  
12 STUART N. LANE<sup>7</sup>, ANDREW P. NICHOLAS<sup>8</sup>, OSCAR ORFEO<sup>9</sup>, STEVEN D. SANDBACH<sup>6,8</sup>,  
13 CHRISTOPHER J SIMPSON<sup>10</sup>, RICARDO N. SZUPIANY<sup>5</sup>  
14  
15  
16  
17  
18  
19

20  
21 *<sup>1</sup>Division of Geography and Geology, School of Environment and Technology, University of*  
22 *Brighton, Brighton, Sussex, BN2 4GJ, UK (E-mail: a.reesink@hull.ac.uk)*  
23

24  
25 *<sup>2</sup>School of Geography, Earth and Environmental Sciences, University of Birmingham,*  
26 *Edgbaston, Birmingham, B15 2TT, UK*  
27

28  
29 *<sup>3</sup>Departments of Geology, Geography and Geographic Information Science, Mechanical*  
30 *Science and Engineering and Ven Te Chow Hydrosystems Laboratory, University of Illinois at*  
31 *Urbana-Champaign, 1301 W. Green St., Urbana, IL, 61801, USA*  
32  
33

34  
35 *<sup>4</sup>Department of Geography, Environment and Earth Sciences, University of Hull, Hull, HU6 7RX,*  
36 *UK*  
37  
38

39  
40 *<sup>5</sup>Universidad Nacional del Litoral, Facultad de Ingeniería y Ciencias Hídricas, Centro*  
41 *Internacional de Estudios de Grandes Ríos, C.C. 217 - (3000) Santa Fe, Argentina*  
42  
43

44  
45 *<sup>6</sup>Department of Geography, Durham University, Durham, DH1 3LE, UK*  
46

47  
48 *<sup>7</sup>Institut de géographie, Faculté des géosciences et l'environnement, Université de Lausanne,*  
49 *Batiment Anthropole, Lausanne, CH2015, Switzerland*  
50

51  
52 *<sup>8</sup>Department of Geography, University of Exeter, Exeter, EX4 4QJ, UK*  
53

54  
55 *<sup>9</sup>Centro de Ecología Aplicada del Litoral, Consejo Nacional de Investigaciones Científicas y*  
56 *Técnicas, Corrientes, Argentina*  
57  
58  
59  
60

Draft paper: Variability in bar sedimentology in a large river, Version 6, 09/03/2011

<sup>10</sup>*Fulcrum Graphic Communications Inc., #1605 – 919 38 Street NE, T2A AB, Calgary, 6E1*

*Canada*

*\*Now at Department of Geography, Environment and Earth Sciences, University of Hull, Hull,*

*HU6 7RX, UK*

## **ABSTRACT**

To date, published studies of alluvial bar architecture in large rivers have been restricted mostly to case studies of individual bars and single locations. Relatively little is known on how the depositional processes and sedimentary architecture of km-scale bars vary within a multi-km reach or over several 100s km downstream. This study presents Ground Penetrating Radar (GPR) and core data from 11, km-scale bars from the Río Paraná, Argentina. The investigated bars are located between 30 km upstream and 540 km downstream of the Río Paraná- Río Paraguay confluence, where a significant volume of fine-grained suspended sediment is introduced into the network.

Bar-scale cross-stratified sets, with lengths and widths up to 600 m and thicknesses up to 12 m, enable the distinction of large river deposits from stacked deposits of smaller rivers, but are only present in half the surface area of the bars. Up to 90% of bar-scale sets are found on top of finer-grained ripple-laminated bar-trough deposits. Bar-scale sets make up as much as 58% of the volume of the deposits in small, incipient mid-channel bars, but this proportion decreases significantly with increasing age and size of the bars. Contrary to what might be expected, a significant proportion of the sedimentary structures found in the Río Paraná is similar in scale to those found in much smaller rivers. In other words, large river deposits are not always

1  
2 characterised by big structures that allow a simple interpretation of river scale. However, the  
3  
4 large scale of the depositional units in big rivers causes small-scale structures, such as ripple  
5  
6 sets, to be grouped in thicker co-sets, which indicate river scale even when no obvious large-  
7  
8 scale sets are present.  
9

10  
11  
12  
13 The results also show that the composition of bars differs between the studied reaches  
14  
15 upstream and downstream of the confluence with the Río Paraguay. Relative to other controls  
16  
17 on downstream fining, the tributary input of fine-grained suspended material from the Río  
18  
19 Paraguay causes a marked change in the composition of the bar deposits. Compared to the  
20  
21 upstream reaches, the sedimentary architecture of the downstream reaches in the top ~5 m of  
22  
23 mid-channel bars shows: (i) an increase in the abundance and thickness (up to m-scale) of  
24  
25 laterally extensive (100s of metres) fine-grained layers; (ii) an increase in the percentage of  
26  
27 deposits comprised of ripple sets (to >40% in the upper bar deposits); and (iii) an increase in  
28  
29 bar-trough deposits and a corresponding decrease in bar-scale cross strata (<10%). The  
30  
31 thalweg deposits of the Río Paraná are composed of dune sets, even directly downstream from  
32  
33 the Río Paraguay where the upper channel deposits are dominantly fine-grained. Thus, the  
34  
35 change in sedimentary facies due to a tributary point-source of fine-grained sediment is  
36  
37 expressed primarily in the composition of the upper bar deposits.  
38  
39  
40  
41  
42  
43  
44  
45

#### 46 **Keywords**

47  
48 Large rivers, bars, dunes, Río Paraná, facies models, GPR, channel deposits  
49  
50  
51  
52  
53  
54  
55  
56  
57  
58  
59  
60

## INTRODUCTION

Although the world's largest rivers dominate the drainage and continental basin sedimentation of the Earth (Potter, 1978; Milliman & Meade, 1983; Schumm & Winkley, 1994; Hovius & Leeder, 1998; Gupta, 2007; Fielding *et al.*, 2012; Lewin & Ashworth, 2012), surprisingly little is known about how these large rivers evolve over time, how they build km-scale bars, whether they produce a characteristic sedimentary architecture, and how this architecture compares to that found in deposits of smaller rivers (Miall & Jones, 2003; Fielding, 2007; Gupta, 2007; Latrubesse, 2008; Sambrook Smith *et al.*, 2009; Ethridge, 2011). Our understanding of large modern rivers underpins our ability to interpret correctly and characterise large rivers in the rock record (Potter, 1978; Miall, 1996; Miall & Jones, 2006; Fielding, 2007; Davidson *et al.*, 2011) and quantify the heterogeneity of large river deposits in fluvial reservoirs (e.g., Hubbard *et al.*, 2011). In addition, the number and function of large rivers is an important variable in geological time because the increase in land area at times of sea-level low-stand causes rivers to merge into large systems that affect long-term variations in the build-up of the continental shelf (Blum *et al.*, 2013). In the present-day channel of the Río Paraná, the dynamics of dunes and bars affect flood heights, control the supply and size of dredged aggregates, control localised erosion and hence damage to infrastructure, determine the navigability of the river, and constrain the physical environment of the biota (Amsler & García, 1997; Amsler & Prendes, 2000; Orfeo & Steveaux, 2002; Amsler *et al.* 2007, 2009; Paoli *et al.*, 2010; Blettler *et al.*, 2012).

Whilst recent studies in large rivers have begun to document the internal architecture of individual, km-scale, mid-channel bars in generally sandy multi-channel rivers (e.g. Bristow, 1993; Steveaux, 1994; Best *et al.*, 2003, 2007; Latrubesse & Franzinelli, 2005; Sambrook Smith *et al.*, 2009; Horn *et al.*, 2012a,b; Valente & Latrubesse, 2012; Rozo *et al.*, 2012), it remains uncertain whether these lithofacies descriptions are representative of the wide range of bar

Draft paper: Variability in bar sedimentology in a large river, Version 6, 09/03/2011

1  
2 types and channel patterns that characterise large rivers (cf. Lewin and Ashworth, 2013;  
3  
4 Nicholas, 2013). For example, little work has been undertaken on how the subsurface alluvial  
5  
6 architecture varies both within a reach, down-river and following mixing with significant tributary  
7  
8 input of fine-grained material (Lane *et al.*, 2008). Past research has shown that sediment load  
9  
10 and grain size may be expected to have a pronounced effect on channel and bar stability (Smith  
11  
12 & Smith, 1980; Federici & Seminara, 2006; Edmonds & Slingerland, 2010; Nicholas, 2013), the  
13  
14 character of flow and bedforms (e.g., Baas *et al.*, 2009; Kostaschuk *et al.*, 2009) and the relative  
15  
16 abundance of small-scale bedforms (Van den Berg & Van Gelder, 1993), yet it is unclear how  
17  
18 these processes affect the heterogeneity of the channel deposits in a large river system with a  
19  
20 significant tributary input of fine-grained sediment.  
21  
22  
23  
24  
25

26 This paper presents data from 40 km of Ground Penetrating Radar (GPR) surveys and 30 cores  
27  
28 collected on eight, km-scale, bars in a 100 km reach of the Upper Río Paraná near Corrientes,  
29  
30 Argentina, and supplementary data from 10 trenches and 11 cores taken on three bars ~540 km  
31  
32 further downstream near Santa Fe (Fig. 1). Additionally, ~350 m of Parametric Echo Sounder  
33  
34 (PES) line are used to illustrate the morphology and composition of the channel bed. The  
35  
36 objectives of this paper are to: (i) describe the origin and evolution of a range of bar types,  
37  
38 morphologies and sizes in this large multi-channel river, (ii) describe and quantify the variability  
39  
40 in alluvial architecture within, and between, bars of different size and origin in a large river, (iii)  
41  
42 determine the influence of a major fine-grained tributary input on the bar sedimentology, and (iv)  
43  
44 compare the sedimentary deposits of the Río Paraná to that of smaller (< 1 km wide) rivers, and  
45  
46 in particular with reference to reservoir properties.  
47  
48  
49  
50  
51  
52  
53  
54  
55  
56  
57  
58  
59  
60

## THE RÍO PARANÁ, ARGENTINA

The Río Paraná is one of the world's largest rivers with a drainage basin of  $2.6 \times 10^6 \text{ km}^2$  (Gupta, 2007; Paoli *et al.*, 2010; Fig 1A). The mean annual water discharge of the Río Paraná at Itati (Fig. 1C) is  $\sim 12,000 \text{ m}^3 \text{ s}^{-1}$ , increasing to  $\sim 17,000 \text{ m}^3 \text{ s}^{-1}$  at Corrientes, 30 km downstream of the confluence with the Río Paraguay (Fig. 1C). Overbank flow upstream of the confluence occurs at  $\sim 19,000 \text{ m}^3 \text{ s}^{-1}$ . Mean annual sediment discharge of the Río Paraná increases from  $\sim 19$  to  $\sim 158 \times 10^6 \text{ tons year}^{-1}$  at the junction with the Río Paraguay, primarily due to the large input of suspended sediment (concentrations between  $600$  and  $1100 \text{ mg L}^{-1}$ ) supplied from the Río Bermejo tributary (Bonetto & Orfeo, 1984; Lane *et al.*, 2008; Amsler & Drago, 2009). Bed material of the upper reach of the Río Paraná is well sorted, predominantly medium-to-fine sand (average  $D_{50}$  of 26 bed samples is  $0.35 \text{ mm}$ ), although some fine gravel is present in the channel thalweg and on aeolian deflation surfaces on some exposed bars. Mean bed grain size downstream of the confluence near Corrientes ranges from  $0.31$  to  $0.45 \text{ mm}$  (Drago & Amsler, 1998; Amsler *et al.*, 2007). Whilst  $\sim 500 \text{ km}$  downstream at Santa Fe (Fig. 1D) the mean bed grain size is  $\sim 0.30 \text{ mm}$ , there is a much higher proportion of fines in the suspended load. Mean slope near Corrientes ranges from  $4.9 \times 10^{-5} \text{ (m/m, bankfull water-surface slope)}$ ; Latrubesse, 2008) to  $8.5 \times 10^{-5} \text{ (m/m, channel slope)}$ ; Orfeo & Steveaux, 2002). The upper reach of the Río Paraná is regulated by a series of large dams (Orfeo & Steveaux, 2002), although the hydrograph is still characterised by floods of long duration that are typically associated with prolonged rainfall in the headwaters during the austral winter. Channel depths in the thalweg vary between  $5$  and  $12 \text{ m}$  with maximum outer bend scours of  $25 \text{ m}$  at discharges of  $\sim 11,000 \text{ m}^3 \text{ s}^{-1}$  (Parsons *et al.*, 2005; Sandbach *et al.*, 2010).

In the studied reach between Itati and Santa Fé, the Río Paraná is a multi-channel river that contains mid-channel bars of unconsolidated sand as well as stable vegetated bars that divide

Draft paper: Variability in bar sedimentology in a large river, Version 6, 09/03/2011

1  
2 flow up to bankfull stage, and could therefore be described as an anabranching river (Nanson &  
3  
4 Knighton, 1996; Latrubesse, 2008; Ashworth & Lewin, 2012). Near Itati (Fig. 1C), the width of  
5  
6 the primary channel ( $1.7 \pm 0.7$  km) is larger than that of the bars ( $0.5 \pm 0.6$  km) and about five  
7  
8 times the width of smaller secondary channels ( $0.3 \pm 0.2$  km). Sandy bars in the Río Paraná are  
9  
10 typically bank-attached, transverse or medial bars (Santos & Steveaux, 2000) with migration  
11  
12 rates of  $\sim 50$  m year<sup>-1</sup>, that reach up to 130 m year<sup>-1</sup> near the Río Paraguay- Río Paraná  
13  
14 junction. Significant portions of the floodplain and stable mid-channel bars are densely  
15  
16 vegetated with mature shrubs and trees, with trees establishing themselves on exposed bars  
17  
18 within decades. The outer bank edges of the primary channel are relatively straight, but a  
19  
20 bathymetric survey of a 38 km reach immediately upstream of the Río Paraná- Río Paraguay  
21  
22 junction shows a dominantly sinuous, meandering thalweg with a wavelength of  $\sim 12$  km  
23  
24 (Ramonell *et al.*, 2002; Sandbach *et al.*, 2012). Outcrops of cemented Pleistocene sediments  
25  
26 are found in places throughout the main study reach, notably on the south-east (left) river bank.  
27  
28 Outcrops can cause local constriction and acceleration of flow and hence accentuate the  
29  
30 deepest thalweg scours against the left bank. The river bed of the Río Paraná is dominated by  
31  
32 dunes at all flow stages (Amsler & Prendes, 2000; Parsons *et al.*, 2005; Kostaschuk *et al.*,  
33  
34 2009; Shugar *et al.*, 2010). Parsons *et al.* (2005) report large dunes with mean heights of 2 m  
35  
36 and wavelengths of 64 m with smaller superimposed dunes with heights up to 0.3 m and  
37  
38 wavelengths up to 10 m in the deeper parts of the channel near Corrientes at a discharge of  
39  
40  $11,000$  m<sup>3</sup> s<sup>-1</sup>. However, much larger dunes with heights up to 6.5 m and wavelengths of 320 m  
41  
42 have been observed in the Río Paraná during the large flood of 1983 (Amsler & Garcia, 1997).  
43  
44 Ripples are present in shallow water and are common on near-emergent bar tops, and aeolian  
45  
46 re-working is widespread on sparsely vegetated, exposed bar tops.  
47  
48  
49  
50  
51  
52  
53  
54  
55  
56  
57  
58  
59  
60



## STUDY REACHES

Data are presented herein from three study sites: (i) a reach from 30 km upstream of the Río Paraná- Río Paraguay confluence to 4 km downstream of the junction, which is not influenced by the fine-grained input from the Río Paraguay; (ii) a reach from 9 km to 74 km downstream of the confluence where the input of fine sediment is more significant, and (iii) a reach much further downstream (520-540 km) near Santa Fe where the Río Paraguay and Río Parana waters are fully mixed (Lane *et al.*, 2008) (Fig. 1, Table 1). Previous descriptions of the Río Paraná near, or within, the upstream study reach are given in Parsons *et al.* (2005, 2007, 2009), Amsler *et al.* (2007), Lane *et al.* (2008), Sambrook Smith *et al.* (2009), Kostaschuk *et al.* (2009), Shugar *et al.* (2010) and Nicholas *et al.*, (2012). Five mid-channel bars were investigated in the upstream study area (Fig. 2A-E, prefix U): three bars were located upstream from the confluence (at distances relative to the Río Paraná- Río Paraguay confluence of -30, -8 and -7.5 km), and two located close to the confluence (at +1 and +4 km downstream) but with only limited influence from the confluence. Three mid-channel bars were studied that were influenced by the confluence (Fig. 2F-H, prefix C) and were located +9, +73 and +74 km downstream of the confluence. Three more bars much further downstream from the confluence (+520 to +537 km; Fig. 2I-K, prefix D) were studied using cores and trenches. The eleven bars were selected to maximise the differences in size, age and location with respect to the Río Paraná- Río Paraguay confluence and to establish any broader upstream-downstream trends (Table 1).

## METHODS

### Ground Penetrating Radar (GPR) surveys

Approximately 40 km of common-offset GPR surveys were collected (Table 1) using a Sensors and Software SmartCart© carrying a Pulse-EKKO PRO system with 100 MHz antennae. Surveys were collected mostly in a rectangular grid except where vegetation blocked access (Fig. 2). Eight stacked traces were collected at every shot point, with the shot points being triggered by the cart's odometer wheel at ~0.1 m spacing. GPR lines were corrected for any topographic variation by interpolation of points ~100 m apart on lines surveyed using a Leica differential Global Positioning System (dGPS) operating in Real-Time Kinematic mode (RTK), which had relative positional errors of  $\pm 0.02$  m horizontally and  $\pm 0.03$  m vertically. Post-processing of the GPR data in Seismic Unix included application of a zero-phase, sine-tapered bandpass filter with polygon frequency values of 10, 50, 250 and 600 MHz. Loss of reflection amplitude with depth was reduced by the application of a time-varying gain. A Stolt-migration based on a single subsurface velocity was applied to reduce the effect of refraction hyperbolae. The radar velocity was determined from Common Mid-Point surveys (CMP's) using normal move-out corrections as well as velocity semblance analyses, and by comparison of the common-offset profiles with core logs. These three different methods yielded consistent results. Two-way travel time was then converted to depth using a constant velocity, derived separately for the bars upstream and downstream of the confluence, of  $0.05 \text{ m ns}^{-1}$  and  $0.08 \text{ m ns}^{-1}$  respectively. The associated wavelengths are in the order of ~0.125 m upstream and ~0.2 m downstream, with maximum vertical resolution a quarter of these wavelengths (Sheriff & Geldart, 1982). The higher radar velocity in the bars downstream from the confluence is attributed to the increase in fine-grained sediment in the deposits (Neal, 2004; Baker *et al.*, 2007). Strong attenuation of the radar signal prevented collection of GPR profiles of sufficient

Draft paper: Variability in bar sedimentology in a large river, Version 6, 09/03/2011

1  
2 depth from the bars near Santa Fe and from those dominated by the influence of the Río  
3  
4 Paraguay (Table 1).  
5  
6  
7

### 8 9 **Classification and description of radar facies**

10 The primary radar facies that characterise the deposits of the Río Paraná in the main study  
11 reach are shown in Table 2. The three key radar facies used here match previous descriptions  
12 of the deposits of a km-scale bar by Sambrook Smith *et al.* (2009), which is bar U4 in the  
13 present study. The only difference herein is that Facies 1 is subcategorised by the angle of  
14 reflections rather than set thickness (Sambrook Smith *et al.*, 2009) because this provides a  
15 better match between the radar reflections and the true sedimentary structures observed in  
16 cores (cores were not available in the earlier study by Sambrook Smith *et al.*, 2009). A brief  
17 description of each radar facies and their sedimentary interpretation is given below and  
18 examples of the radar facies are shown in Table 2 and Fig. 3.  
19  
20  
21  
22  
23  
24  
25  
26  
27  
28  
29  
30  
31  
32

#### 33 **(1A) Large-scale high-angle and (1B) medium-angle inclined reflections**

34 Facies 1 is characterised by sets of dipping reflections with angles  $>6^\circ$ . Sets of facies 1 can  
35 commonly be traced laterally for several hundreds of metres (up to 600 m) and have  
36 thicknesses of 2 m on average with a maximum observed thickness of 12 m. The study herein  
37 subdivides radar facies 1 into high-angle (1A; Table 2; Fig. 3A, C-D, G-H) and medium-angle  
38 (1B; Table 2; Fig. 3A-C, E-H) reflections. Large-scale (cf. Bridge, 1993a), high-angle reflections  
39 (facies 1A) exceed  $20^\circ$  and are characteristically straight with low amplitudes. Large-scale,  
40 medium-angle reflections (facies 1B) vary in angle between  $6^\circ$  and  $20^\circ$  and are typically more  
41 irregular in shape with higher amplitudes. Facies 1A is associated primarily with angle-of-repose  
42 cross-strata formed by grainflows on large-scale dune or bar slopes (Reesink & Bridge, 2007,  
43 2009) and may include compound reflections (Reesink & Bridge, 2011). Facies 1B represents  
44  
45  
46  
47  
48  
49  
50  
51  
52  
53  
54  
55  
56  
57  
58  
59  
60

1  
2 large-scale inclined co-sets: stacks of inclined small- and medium-scale sets. Such co-sets are  
3  
4 interpreted as formed by ripples and dunes migrating over steep topography (e.g. a unit-bar lee  
5  
6 slope; [Haszeldine, 1982](#)). Thus, both facies 1A and B represent bar-margin accretion, and are  
7  
8 consequently commonly observed adjacent to one another and grading into one another ([Fig.](#)  
9  
10 [3A, C, H, label I](#)).

## 15 **(2) Near-horizontal, undular, discontinuous and chaotic reflections**

17 Facies 2 ([Fig. 3A-B, D-G, label 2](#)) is composed of near-horizontal ( $<6^\circ$ ) reflections that may be  
18  
19 chaotic ([Fig. 3C, F, label II](#)), discontinuous ([Fig. 3C, E, label III](#)) or contain m-scale trough  
20  
21 shapes (e.g. [Fig. 3A, label IV](#)). The lateral extent of these reflections is less than 60 m and  
22  
23 amplitudes are not usually higher relative to surrounding reflections. The symmetry and  
24  
25 continuity of the reflections in facies 2 are highly variable and typically grade both laterally and  
26  
27 vertically. Trough-shaped reflections within facies 2 are up to 2 m high and 50 m long, less than  
28  
29 the thicknesses and lengths of sets of facies 1. These trough-shapes are primarily attributed to  
30  
31 the trough-shapes of dune sets. Facies 2 also includes asymmetrical reflections that resemble  
32  
33 complete dune profiles ([Fig. 3E-F, label V](#)), and are interpreted as trains of dunes that were  
34  
35 abandoned and did not undergo any great reworking before being buried under subsequent  
36  
37 sediment. Facies 2 includes reflections from both the individual bounding surfaces of sets with  
38  
39 sizes larger than the radar wavelength (dunes, small unit bars) and reflections that relate to  
40  
41 grain-size variations within stacks of sets smaller than the radar wavelength (ripples, small  
42  
43 dunes). Thus, facies 2 is associated with near-horizontal medium- and small-scale sets that are  
44  
45 attributed to dunes and ripples respectively.  
46  
47  
48  
49  
50  
51  
52  
53  
54  
55  
56  
57  
58  
59  
60

### (3) Laterally-extensive, high-amplitude reflections

Facies 3 comprises laterally-extensive reflections (up to 1 km and approaching the lengths of the bars) that have distinctively higher amplitudes relative to adjacent reflections (Fig. 3A-H, label 3). Facies 3 is commonly associated with loss of the radar signal below the reflection. These reflections represent laterally-extensive bounding surfaces within the bars that are primarily transitions from relatively coarse-grained bar-margin deposits (mean 0.33 mm in cores) to underlying layers of finer-grained ripple-sets (mean 0.18 mm in cores), with limited thicknesses, which are deposited in the bar troughs and during low-flows. The distinct contrast in grain size at the top of the fine-grained bounding surfaces generates high-amplitude GPR reflections, with the observed loss in radar amplitude directly underneath these high-amplitude reflections being associated with attenuation of the signal by fine-grained sediment such as clay (Neal, 2004; Baker *et al.*, 2007).

#### Calculation of facies distribution

All GPR data were interpreted as illustrated in Fig. 3H, with reflections assigned a facies classification based on the criteria outlined above and summarised in Table 2. The radar facies were identified from vertical profiles, and these data were then used to calculate the mean, standard deviation and distribution of the facies (% of all facies that were identified in the GPR images from different locations, hence representing a volume) and the presence/absence of facies (expressed as a percentage of the bar area investigated). Maps of facies distributions were constructed by spatial averaging using a 200 x 200 m square window (i.e. larger than the spacing of the survey lines) (Fig. 4). The thickness of the reflections associated with facies 3 has been determined from the cores in this study because GPR alone does not provide accurate measurements of the thickness of fine-grained layers, since these are of the same order of magnitude as the radar wavelength. The mean thickness of silts and very-fine sands

1  
2 (0.2 ±0.2 m) from the core observations is therefore used to quantify and estimate the  
3  
4 proportion of fine-grained layers represented by facies 3 in the GPR images.  
5  
6  
7

## 8 **Coring**

9  
10 In order to ground-truth the GPR and provide information on the sedimentary architecture of the  
11  
12 deposits at resolutions higher than provided by the GPR, 30 cores of the bar sediments were  
13  
14 taken on GPR lines. Cores were obtained using a modified Van der Staay suction corer with a  
15  
16 diameter of 0.06 m (Van de Meene *et al.*, 1979; see Fig. 2; Table 1). In addition, 11 cores were  
17  
18 taken from mid-channel bars near Santa Fé (Fig. 1D) in order to sample the bar deposits where  
19  
20 the water and sediment of the Río Paraguay are more fully mixed with that of the Río Paraná  
21  
22 and where GPR provided no data. Van der Staay suction coring works well in sand, but did not  
23  
24 work well in deposits that were dominated by silt and clay. Cores retrieved from the sandy bars  
25  
26 had an average length of 4 m and a combined length of 149.3 m. The cores were sawn in half  
27  
28 lengthwise and epoxy peels made of one half. Sediment-samples were taken from selected  
29  
30 locations within the cores and grain-size distributions determined by dry sieving and grain sizing  
31  
32 obtained using a Malvern Laser Mastersizer 2000. Detailed logs of the sedimentary structures  
33  
34 were constructed by analysis of the epoxy peels following the methodology outlined by Bridge  
35  
36 (2003) (Fig. 5, Fig. 10).  
37  
38  
39  
40  
41  
42  
43

## 44 **Parametric Echo Sounder (PES)**

45  
46 To establish if these facies observed in the GPR from the bars are representative of sediments  
47  
48 lower down within the profile, an Innomar<sup>TM</sup> (SES-2000 light) Parametric Echo Sounder (PES)  
49  
50 was used to undertake a preliminary survey in the channel adjacent to C1. The principles of the  
51  
52 PES are described fully by Wunderlich and Müller (2003) and Sambrook Smith *et al.* (2013), but  
53  
54 in brief, its most important feature is an ability to generate a broad array of acoustic frequencies;  
55  
56  
57  
58  
59  
60

Draft paper: Variability in bar sedimentology in a large river, Version 6, 09/03/2011

1  
2 the lower frequencies provide details of the subsurface structure while the higher frequencies  
3  
4 are able to record the bed surface as is standard for common echo-sounders. Although this  
5  
6 acoustic-based technique is fundamentally different from the electromagnetic based GPR  
7  
8 technique, the reflections generated by contrasting sediment strata generate similar facies  
9  
10 (Table 2). In this study, the subsurface PES reflections are used to show the bounding surfaces  
11  
12 of preserved sets below the active dune forms in the channel.  
13  
14  
15  
16

## 17 RESULTS

18  
19 The development and approximate age of the investigated bars (Fig. 2) were established from  
20  
21 their appearance in Landsat images (Band 1-3) that were taken between 1972 and 2010 (Fig.  
22  
23 6). The composition of the bars observed in the GPR images (Figs 3, 7 and 8) and cores (Figs 5  
24  
25 and 10) is expressed as maps of frequency of occurrence of different facies (Fig. 4). The results  
26  
27 are summarised in Table 1 and a description of bar composition and its relation to bar  
28  
29 development is given below.  
30  
31  
32  
33  
34

### 35 *Evidence from GPR*

36  
37 Overall, facies 1A, 1B, 2, and 3 make up ~20, 17, 56 and 7 % of the entire investigated volume.  
38  
39 Most studies suggest that small- and medium-scale sets, and in particular dune sets, are the  
40  
41 most abundant sedimentary structures in bars within multi-channel rivers (e.g. Best *et al.*, 2003;  
42  
43 Skelly *et al.*, 2003; Bridge & Lunt, 2006; Sambrook Smith *et al.*, 2006; Bridge, 2009; Ethridge,  
44  
45 2011). These structures are included here in Facies 2 and 1B, which indeed make up the  
46  
47 majority of the investigated deposits. In contrast to the volumetric analysis, 2D spatial analysis  
48  
49 shows that, whereas facies 2 and 3 are found in nearly the entire investigated area (97 and  
50  
51 98%; Fig. 9), the bar-margin deposits represented by facies 1A and 1B are found in only  
52  
53 approximately half (45 and 49%) of the investigated area.  
54  
55  
56  
57  
58  
59  
60

1  
2  
3  
4 Subdivision of the results per bar shows that the mean volumes of facies 1A, 1B, 2 and 3 range  
5  
6 between 4-58, 0-48, 38-70, and 2-12% for different bars (Fig. 9). In contrast, the areal coverage  
7  
8 of facies 1A, 1B, 2 and 3 ranged between 8-100, 0-90, 87-100 and 92-100% respectively.  
9  
10 Facies 2 comprises most of the deposits and is ubiquitous. Facies 3 is also found nearly  
11  
12 everywhere, but represents only a small proportion of the sediments. Facies 1A and 1B, which  
13  
14 represent horizontal progradation of bar margins, may comprise up to half of the volume of a  
15  
16 bar, but are spatially limited in their extent (Fig. 4). These spatial contrasts in bar composition  
17  
18 can be associated with the nature of bar development (Table 1).  
19  
20  
21  
22  
23

24 Facies 1A and 1B are particularly prominent in the newly-emergent incipient bars (e.g. for U3:  
25  
26 1A is 58% of volume and 100% of area). Large-scale sets of facies 1A and 1B were also  
27  
28 present lower down in the centre of the larger bars (U2 and U4). Analysis of satellite images  
29  
30 (Fig. 6A-C) confirms that these sets formed by downstream-migrating bar margins during the  
31  
32 earlier stages of bar development. These observations suggest that the downstream migration  
33  
34 and amalgamation of unit bars is common in the early stages of bar development.  
35  
36  
37  
38  
39

40 Although facies 1 was also prominent near visible large-scale slopes at the tails of the larger,  
41  
42 older bars (U1, U2 and U4; Fig. 4), two of the larger, older bars (U5 and C2) had no significant  
43  
44 bar-tail sets >1 m thick but possessed low-angle slopes at the edge of the bars that represent a  
45  
46 record of more gradual, vertical aggradation. Thus, although continued growth by horizontal  
47  
48 progradation of bar-scale slopes is possible (e.g. large set in U1 and bar tails in U1, U2 and  
49  
50 U4), the style of deposition may change during a development of a bar to include increased  
51  
52 proportions of vertical aggradation (Bristow, 1987). Bar U1 represents an extreme example of  
53  
54  
55  
56  
57  
58  
59  
60



Draft paper: Variability in bar sedimentology in a large river, Version 6, 09/03/2011

1  
2 such differing styles of composition: the right half of U1 formed by a migrating bar front and the  
3  
4 left half formed by in-situ vertical aggradation (Fig. 4; Fig. 5A,B).  
5  
6  
7

8  
9 Vertical associations of the facies indicate that facies 1A and 1B are mostly underlain by facies  
10  
11 3 (91, 80%; Table 3). This preferential association indicates that channel deposits  
12  
13 characteristically comprise bar-scale sets with laterally-extensive fine-grained bottomsets at  
14  
15 their base (Fig. 5D, F; Fig. 10E, F). Although facies 1A and 1B are nearly always underlain by  
16  
17 facies 3, facies 3 is also found in association with facies 2 (66 percent). Clearly, fine-grained  
18  
19 bounding surfaces can have different origins (e.g. low-flow deposits) and need not be formed  
20  
21 and preserved uniquely in the bar troughs. The observed reduction in the volumetric abundance  
22  
23 of facies 1A downstream from the confluence (C1-3; only 4% of the deposits) may be caused  
24  
25 partially by an increase in fine-grained bar-trough deposits. Finer-grained sediment is carried  
26  
27 further beyond the brink point of bedforms and is commonly deposited on low-angle slopes  
28  
29 (Facies 1B; 48% in C3) and in the trough (Boersma, 1967; Jopling, 1965). Such a relative  
30  
31 increase in trough deposits and low-angle slopes is matched by a corresponding decrease in  
32  
33 facies 1A.  
34  
35  
36  
37  
38

#### 39 *Evidence from cores*

40  
41  
42 Cores from the upper 5 m of the deposits support observations from the GPR in showing a wide  
43  
44 diversity of structures within individual bars and an excellent agreement between GPR  
45  
46 reflections and the sedimentary structures. When viewed as a downstream transition from the  
47  
48 upstream bars (U1-U5) above the Río Paraguay confluence to those just downstream of it (C1-  
49  
50 C3) and much further away (D1-3), some clear trends can be identified in the bar-top sediments  
51  
52 from these cores (Table 5). The downstream bars have a larger proportion of ripple sets (mean  
53  
54 43%, range 15-56%) in comparison to the upstream bars (mean 31%, range 2-43%) and the  
55  
56  
57  
58  
59  
60

Draft paper: Variability in bar sedimentology in a large river, Version 6, 09/03/2011

1  
2 proportion of dune and bar sets is smaller in the downstream bars (mean 32%, range 19-42%)  
3  
4 relative to the upstream bars (mean 47%, range 21-98%). This difference in larger-scale sets  
5  
6 matches to the lower abundance of bar sets in the GPR of the downstream bars (Bars C2,3,  
7  
8 [Table 1](#)), which comprise 8% of the downstream deposits and 20% of the upstream deposits  
9  
10 ([Fig. 9](#)). In addition to differences in the relative proportions of sedimentary structures, grain size  
11  
12 analyses show that the downstream cores and trenches contain a larger proportion of fine-  
13  
14 grained material ([Table 4](#)). Grain size distributions are typically >90% sand with  $D_{50} > 250 \mu\text{m}$  in  
15  
16 the upstream sites where there is no influence from the input of fines from the Río Paraguay.  
17  
18 Where the waters of the two rivers become well mixed downstream of the junction, the  
19  
20 percentage of silt/clay in the bar sediments can reach 31% with a  $D_{50}$  as low as 141  $\mu\text{m}$ . This  
21  
22 increased proportion of fine-grained sediment is found throughout the deposits in the bar-tops  
23  
24 and occurs both as local deposits of several metres thickness and interbedded with coarser-  
25  
26 grained bedload-dominated deposits ([Fig. 10A, C, D](#)). The increased occurrence of interbedded  
27  
28 fine and coarse deposits is illustrated by the greater number of dunes that occur as solitary sets,  
29  
30 and interbedded with other structures instead of in stacks of dune sets in the bar-top sediments  
31  
32 (e.g. [Figs 5 and 10A](#)). Whereas only 15% of the dune sets in the upstream reach are found as  
33  
34 solitary sets or interbedded with other sedimentary structures, this proportion rises to 35% in the  
35  
36 downstream reach. The increased deposition of fines therefore increases the heterogeneity of  
37  
38 the deposits and reduces the number of dunes in co-sets in the upper portions of channel fill/bar  
39  
40 sequences.  
41  
42  
43  
44  
45  
46  
47  
48

49 *Additional evidence of channel deposits: Parametric Echo Sounder (PES)*

50 Because of the limited depth of the cores and GPR penetration in some locations, the  
51  
52 information contained in the current dataset has a bias towards the upper bar deposits. The  
53  
54 persistent presence of dunes in the deeper parts of the channel ([Amsler & García, 1997](#); [Drago](#)  
55  
56  
57  
58  
59  
60

Draft paper: Variability in bar sedimentology in a large river, Version 6, 09/03/2011

1  
2 & Amsler, 1998; Amsler & Prendes, 2000; Parsons *et al.*, 2005; Amsler *et al.*, 2007; Kostaschuk  
3  
4 *et al.*, 2009; Shugar *et al.*, 2010) does provide some evidence to infer that dune sets may be  
5  
6 abundant in the lower parts of the deposits of the Río Paraná. Yet, in the absence of subsurface  
7  
8 data, such inference provides only a suggestion. For example, GPR was unsuccessful at bar  
9  
10 C1, and repeated coring attempts indicated that the upper 5.5 metres were composed of very  
11  
12 soft silt and mud. The only core retrieved from the coarser-grained bar head of C1 is composed  
13  
14 primarily of ripple-sets. Thus, the upper bar deposits are dominantly fine-grained and ripple-  
15  
16 laminated. The PES survey shown in Fig. 11 (see Sambrook Smith *et al.*, 2013 for more details)  
17  
18 indicates that the channel bed is dominated by dunes 1-2 m high with smaller superimposed  
19  
20 bedforms on their stoss slopes of ~0.2 m height. Distinct dune sets visible in the PES images  
21  
22 show sets with thicknesses in the order of 0.3 and up to 1.5 m. The PES reflections show that  
23  
24 the thalweg deposits in the reach that is most strongly influenced by fine sediment input from  
25  
26 the Río Paraguay are also composed of dune sets, and hence are comparable to the deposits  
27  
28 of the sandier upstream reach. Clearly, the fine-grained bar tops observed in the field contrast  
29  
30 with the deposits of the adjacent thalweg observed by the PES. Thus, the sudden increase in  
31  
32 fine-grained sediment from the Río Paraguay confluence is expressed in a structural change in  
33  
34 the bar top deposits, but does not necessarily change the nature of the thalweg deposits.  
35  
36  
37  
38  
39  
40  
41

## 42 DISCUSSION

### 43 *Heterogeneity of large river deposits*

44  
45  
46 As Miall (2006) and Fielding (2007) highlight, the lack of sedimentological data from large rivers  
47  
48 has meant there are no universally-accepted criteria for the recognition of their deposits in the  
49  
50 rock record. However, both Miall (2006) and Fielding (2007) point out that the vertical  
51  
52 dimensions of cross-stratification can be a useful indicator of large rivers. This suggestion is  
53  
54  
55  
56  
57  
58  
59  
60

1 supported by the GPR studies of single bars in the Jamuna River (Best *et al.*, 2003) and Río  
2 Paraná (Sambrook Smith *et al.*, 2009) where thick sets of bar-margin facies (radar facies 1A in  
3 this paper) were reported of 8 m and 6 m respectively. Likewise, in one of the most commonly  
4 quoted examples of large river deposits preserved in outcrop, the Hawkesbury Sandstone, Miall  
5 and Jones (2003) report that cross-stratified sets of 2-3 m thickness are common with a  
6 maximum of 7 m. The GPR data in this study confirm that cross-stratified sets with average  
7 thicknesses of 2 m and up to 12 m are common, comprising up to 20% of the overall deposits.  
8 Thick cross-stratified sets were readily identified in cores (Figs 5A, D, E and 9E) and can be  
9 used as indicators of river scale. However, this study also revealed an abundance of  
10 sedimentary structures with scales similar to those found in smaller rivers and a high degree of  
11 variability and clustering of structures within the deposits. This heterogeneity poses a significant  
12 obstacle to interpretations of scale and sedimentary composition of river deposits, which  
13 underpin facies models, palaeo-environmental interpretations, and predictions of permeability,  
14 porosity and connectivity of sandstone reservoirs and aquifers. The present paper is based on a  
15 much broader range of bars than previous studies and therefore permits a fuller consideration of  
16 the scales and causes of heterogeneity in bar deposits in the Río Paraná. The sedimentology of  
17 the deposits investigated varies (i) within bars, (ii) between bars of varying morphology, size  
18 and history, and (iii) as a result of a major fine-grained tributary input. These factors and (iv) the  
19 similarity with smaller river systems, in particular with reference to reservoir properties, are  
20 discussed below.

#### *Variability within bars: systematic clustering of facies*

21 A key point to emerge from the results presented herein is that the presence of thick cross-  
22 stratified sets, which is diagnostic in interpretations of river scale, is spatially-restricted.  
23 Although radar facies 1A and 1B locally dominate bar composition, their presence is restricted

Draft paper: Variability in bar sedimentology in a large river, Version 6, 09/03/2011

1  
2 spatially to roughly half the investigated area (Figs 4, 5 and 9). Thus, although a sample section  
3  
4 may have no diagnostic, thick cross-stratified sets, this does not imply that the deposits are not  
5  
6 related to a large river. This point is illustrated by the contrasting structures found in two cores  
7  
8 from the upstream bar U1 (Figs 2A and 5A-B). While one core displays a thick set of facies 1  
9  
10 associated with migration of a bar lee slope (Fig. 5A), the other shows pervasive ripple sets  
11  
12 associated with slower flow in the lee of the bar (Fig. 5B). Fortunately, the presence of this and  
13  
14 other thick ripple co-sets suggests that the size of large-scale depositional units, other than bar-  
15  
16 scale cross-strata, can also be used to indicate river scale. Similar to large-scale sets, the  
17  
18 thickness of ripple co-sets relates to the distribution of large-scale depositional units, which is an  
19  
20 indicator of river scale. River deposits are generally considered to be composed of a limited  
21  
22 number of large-scale depositional units (Bridge, 1993b, 2003) and this characteristic is  
23  
24 supported by the GPR analysis in this study (Fig. 7). The stacking of a limited number of large-  
25  
26 scale units appears scale-independent (Fielding, 2007), and pronounced spatial clustering of  
27  
28 sedimentary facies related to bar morphology has also been observed in much smaller rivers  
29  
30 (Sambrook Smith *et al.*, 2006; Horn *et al.*, 2012a,b).  
31  
32  
33  
34  
35  
36

### 37 *Variability between bars: effects of bar evolution*

38  
39 The most relevant comparison here is between bars U1, U2 and U3 as these are all located in  
40  
41 the same reach, are active sandy bars with little vegetation cover and have similar grid-based  
42  
43 GPR datasets. Hence all aspects of within-bar variability, discussed above, should be  
44  
45 accounted for. Figure 9 shows that there is a systematic decrease in the percentage of facies  
46  
47 1A between bars U1-U3, from 20%, to 27% and then 58% with increasing age and size. The  
48  
49 Landsat images (Fig. 6A-B) show that bars U1 to U3 vary in age, with U1 and U2 being much  
50  
51 older and larger than U3 (Table 1). Based on an analysis of several rivers, Sambrook Smith *et al.*  
52  
53 (2009) and Parker *et al.* (2013) suggested that the time scale over which bars develop would  
54  
55  
56  
57  
58  
59  
60

1  
2 influence their facies distributions, and this conclusion is supported herein. Small incipient bars  
3  
4 with a simple morphology and a short history of development, such as U3, are dominated by  
5  
6 facies 1. As bars grow and age, the abundance of facies 1 in the bars decreases (e.g. U3 and  
7  
8 U2). This proportional decrease in the occurrence of bar-scale cross strata is attributed to  
9  
10 erosion of the original bar-scale set, and/or, to further deposition of smaller-scale sets by ripples  
11  
12 and dunes as bars grow in time. Consequently, larger bars are composed of a mosaic of  
13  
14 different types of structures and, relative to their larger size, include a larger proportion of small-  
15  
16 and medium-scale sets. Thus, the angle-of-repose bar-scale sets of the incipient bars are  
17  
18 progressively reworked, and bar compositions reflect an increasing range of temporal and  
19  
20 spatial boundary conditions as the bars grow and evolve over time.  
21  
22  
23  
24  
25

26 *Variability between reaches: effects of a fine-grained tributary input*

27  
28 Downstream variability in the alluvial architecture of large sand-bed rivers over distances of  
29  
30 hundreds of kilometres and including the effects of tributary inputs has not been studied  
31  
32 extensively. However, examples from the Rhine, Mississippi and Ganges rivers suggest that  
33  
34 subtle, downstream fining in large sand bed rivers is a common phenomenon (Frings, 2008).  
35  
36 For example, for the Ganges River, Singh et al. (2007) demonstrate that over approximately  
37  
38 2000 km, the grain size distribution of this sand-bed river changes from predominantly medium  
39  
40 and fine sand upstream to fine sand, very fine sand and silt/clay downstream. Conversely, the  
41  
42 grain-size differences between the reaches investigated in the Río Paraná can, for a large part,  
43  
44 be attributed to the tributary input of the Río Paraguay (Table 4). Assessment of the effect of  
45  
46 this input of fine-grained sediment on the bar sedimentology is complicated by the inherent  
47  
48 variability of the deposits, which relates to the location within a bar and the age of the bar as  
49  
50 discussed above. In addition, the onset of any changes in sedimentary composition varies as a  
51  
52 function of the dynamics that control the mixing of the sediment from the Río Paraná and Río  
53  
54  
55  
56  
57  
58  
59  
60

Draft paper: Variability in bar sedimentology in a large river, Version 6, 09/03/2011

1  
2 Paraguay (Lane et al., 2008). GPR data from bars C2 and C3, located at 73 and 74 km  
3  
4 downstream from the confluence, still yield viable GPR data that indicate a change in  
5  
6 proportional composition relative to the upstream bars (Table 1, Figs 4 and 9). At >520 km  
7  
8 downstream, near Santa Fé, the evidence from the bars is restricted mostly to the upper bar  
9  
10 deposits (25-33% of the upper bar/channel fill sequence) because GPR surveys near Santa Fe  
11  
12 (bars D1-D3) were not possible. The interpretations from this area are based on shallow cores  
13  
14 and trenches, although it is noted that consistent attenuation of the radar signal itself also  
15  
16 provides an important clue as to the composition of the upper bar deposits. The most prominent  
17  
18 changes in sedimentary architecture in the bar-top sediments near Santa Fé relate to the  
19  
20 introduction of fine-grained material from the Río Paraguay:  
21  
22

- 23 1) an increased proportion of ripple sets (> 40% of deposits), both as thick co-sets and  
24  
25 interbedded with other sedimentary structures  
26  
27
- 28 2) a decrease of unit-bar foresets (< 10% of deposits) relative to unit-bar trough deposits  
29  
30
- 31 3) an increase in the abundance (> 10% silt/clay in grain size distribution) and thickness of  
32  
33 fine-grained sediment layers (up to several metres thick), many of which are likely to  
34  
35 have a bar-scale extent.  
36

37 Although thick sets of cross-strata (i.e. facies 1A) normally provide a focus with respect to the  
38  
39 deposits of large rivers, one of the most striking features of the cores presented herein is the  
40  
41 relative abundance of ripple sets within the upper 4-5 m of the bar deposits (Table 5). Large  
42  
43 proportions of ripple-sets are also found in the upstream reach, but are related to localised flow  
44  
45 deceleration in response to the morphological development of the mid-channel bars. In the  
46  
47 downstream reach, the presence of ripple-sets is far more pervasive throughout the upper bar  
48  
49 deposits and is also found in the troughs of individual dune sets.  
50  
51  
52  
53  
54  
55  
56  
57  
58  
59  
60

### *Comparison with smaller rivers and effects on reservoir properties*

The variability of facies in the bars investigated herein has many similarities to that described from much smaller rivers (Allen, 1983; Skelly *et al.*, 2003; Lunt & Bridge, 2004; Sambrook Smith *et al.*, 2006; Horn *et al.*, 2012a,b), where channel deposits are also composed of a limited number of large-scale depositional units and where bar morphology also results in pronounced spatial clustering of the sedimentary facies. This potential scale-independent character of the large-scale architecture (cf. Fielding, 2007) does not imply a similarity in the relative abundance of large-scale elements, nor of sedimentary structures within them, as these are known to vary significantly between different systems (Hickin, 1993; Miall, 1996; Bridge, 2009).

The persistent presence of facies 3 as the bounding layers that delineate the large-scale units within the bars compares to observations from smaller river systems and has significant implications for the connectivity of the higher-permeability elements within the deposits. Channel-scale, laterally-continuous, fine-grained deposits are observed in cutbanks near Santa Fe (e.g., Fig. 10C), and in the cores (Figs 5 and 10F) and radar facies 3 in the GPR images (e.g. Figs 3 and 7). Larue and Hovadik (2006) discuss how connectivity within a reservoir can be reduced by compartmentalization associated with local muddy deposits, specifically where: (1) a mud drape covers the channel base, (2) laterally-continuous horizontal muds are located within a channel, and (3) inclined mud units are found (e.g. Lynds & Hajek, 2006; Martinus & Van den Berg, 2010). The dominant association of facies 1 (unit-bar sets) with underlying finer-grained layers in both the upstream and downstream reaches (Table 3; Fig. 5D,F; Fig. 10F) suggests that stacking of unit-bar deposits may play a key role in the development of baffles to flow that could ultimately reduce reservoir connectivity in channel deposits. In addition, the increased abundance of fine-grained layers found downstream from the confluence with the Río Paraguay implies that such a significant point-source change in a large river system with a long



Draft paper: Variability in bar sedimentology in a large river, Version 6, 09/03/2011

1  
2 downstream-fining distance (cf. Frings, 2008) may result in a marked, and potentially spatially  
3  
4 rapid, change in reservoir quality.  
5  
6  
7

8  
9 Finally, the present study identifies multiple controls on the variability in sedimentary  
10 heterogeneity and highlights the different spatial scales at which they occur. Locally, individual  
11 bars produce sedimentary architectures that are unique to the local flow and sediment transport  
12 conditions and that reflect their evolutionary history. In addition, this investigation, of multiple  
13 bars along a 570 km long reach, allowed an assessment of larger, reach-scale changes in  
14 boundary conditions. At such reach scales, the sedimentary composition was shown to change  
15 abruptly in response to a local point-source input in fine-grained sediment, and gradually in  
16 response to more gradual changes in the mixing of waters. It is well-known that sedimentary  
17 heterogeneity within bar deposits varies over a range of scales, yet few of the causes have  
18 been highlighted to date. In this study, the variability in sedimentary heterogeneity within and  
19 between bars is attributed to their age, size, shape and evolutionary history, and the variability  
20 between different reaches is attributed to a tributary input and mixing dynamics of two confluent  
21 flows (Lane *et al.*, 2008).  
22  
23  
24  
25  
26  
27  
28  
29  
30  
31  
32  
33  
34  
35  
36  
37  
38  
39

## 40 CONCLUSIONS

41 Ground Penetrating Radar and core data from 11, km-scale bars over a ~600 km downstream  
42 length of the Río Paraná show that the channel deposits are composed of three principal GPR  
43 facies. Facies 1 represents bar-scale sets with heights up to 12 m and lengths up to 600 m that  
44 are internally composed of angle-of-repose cross strata (Facies 1A: 8-58% of the investigated  
45 volume) or inclined dune- and ripple co-sets (Facies 1B: 0-48%). Facies 2 represents significant  
46 volumes of near-horizontal dune and ripple-scale sets (32-60%). Facies 3 represents laterally-  
47 extensive layers of finer-grained ripple sets (2-12%). Four principal conclusions can be made:  
48  
49  
50  
51  
52  
53  
54  
55  
56  
57  
58  
59  
60

Draft paper: Variability in bar sedimentology in a large river, Version 6, 09/03/2011

- 1  
2  
3  
4  
5  
6  
7  
8  
9  
10  
11  
12  
13  
14  
15  
16  
17  
18  
19  
20  
21  
22  
23  
24  
25  
26  
27  
28  
29  
30  
31  
32  
33  
34  
35  
36  
37  
38  
39  
40  
41  
42  
43  
44  
45  
46  
47  
48  
49  
50  
51  
52  
53  
54  
55  
56  
57  
58  
59  
60  
1) Between 32 and 91% of the investigated depositional structures of the Río Paraná are similar in scale to that found in smaller rivers. In other words, large river deposits are not characterised consistently by large sedimentary structures that facilitate a straightforward interpretation of river scale. However, many of the smaller dune- and ripple sets are stacked in thick co-sets that do scale to river size.
- 2) Bar-scale cross-strata and bar-scale inclined co-sets (Facies 1A and B) are found overwhelmingly on top of layers of finer-grained ripple-sets (Facies 3) that are deposited in the lee of migrating bars. The systematic presence of these laterally-extensive fine-grained layers will limit the connectivity of depositional units with higher permeabilities.
- 3) The bar-scale sets with angle-of-repose cross strata (Facies 1A), which are the most reliable indicators of the size of a river, are restricted spatially to half of the bar-surface area and occur predominantly in the smaller, more recently formed bars. This reduction of bar-scale cross-strata in older and larger bars is attributed to a combination of reworking and changes in the styles of accretion as the bars evolve over time.
- 4) Relative to other controls on downstream fining, the point-source input of fine-grained sediment from the Río Paraguay causes most change to the upper bar deposits. The increased presence of fines manifests itself as i) an increased abundance, and thickness, of laterally-extensive fine-grained layers, ii) an increased abundance of ripple sets, and iii) as a proportional reduction of bar-scale angle-of-repose cross strata. In contrast to the bar-top deposits, the thalweg of the Río Paraná is characterised by metre-scale dunes, and its deposits are composed of dune sets even in areas where bar-top deposits are dominantly fine-grained. Thus, changes in the sedimentary architecture and permeability characteristics of km-scale bars due to a fine-grained tributary input are expressed primarily in the composition of the bar-top deposits.

## ACKNOWLEDGMENTS

This research was supported by grant NE/E016022/1 from the UK Natural Environment Research Council (NERC). The Parametric Echo Sounder data were provided through funding from the Threet Chair in Sedimentary Geology and University of Illinois to JLB and NERC grant NE/I015876/1 awarded to GHSS. We are grateful for the help from staff at CECOAL-CONICET (Corrientes, Argentina), INALI-CONICET (Santa Fe, Argentina), and FICH (Santa Fe, Argentina), and in particular Casimiro Roberto, Christine Sinclair, Juan Jose Neiff, Mir Roberto, Estafan Creus, Lordi Eduardo, Juan and Santiago Cañete. Club Nautico Paraná is thanked for giving access to their marina and provision of overnight mooring in Santa Fe. Reviews by Chris Fielding, Rob Duller and editor Steve Rice are gratefully acknowledged.

## REFERENCES

- Allen, J.R.L.** (1983) Studies in Fluvial Sedimentation – Bars, bar-complexes and sandstone sheets (low sinuosity braided streams) in the Brownstones (L-Devonian), Welsh Borders. *Sedimentary Geology*, **33** (4), 237-293.
- Amsler, M.L. and Drago, E.C.** (2009) A review of the suspended sediment budget at the confluence of the Parana and Paraguay Rivers. *Hydrological Processes*, **23**, 3230-3235.
- Amsler, M.L. and Garcia, M.H.** (1997) Sand-dune geometry of large rivers during floods - Discussion. *Journal of Hydraulic Engineering - ASCE*, **123**, 582-585.
- Amsler, M.L. and Prendes, H.H.** (2000) Transporte de sedimentos y procesos fluviales asociados. In: *Contribución al conocimiento y prácticas ingenieriles en un grande río llanura* (Eds C. Paoli and M.I. Schreider), Centro de Publicaciones, Universidad Nacional del Litoral, 233-306.

Draft paper: Variability in bar sedimentology in a large river, Version 6, 09/03/2011

1  
2 **Amsler, M.L., Drago, E.C. and Paira, A.R.** (2007) Fluvial sediments: Main channel and  
3 floodplain interrelationships. In: *The Middle Parana River* (Eds I. M.H., J.C. Paggi and M.J.  
4 Parma).  
5  
6

7  
8 **Amsler, M.L., Blettler, M.C.M., and Drago, I.E.** (2009) Influence of hydraulic conditions over  
9 dunes on the distribution of the benthic macroinvertebrates in a large sand bed river. *Water*  
10 *Resources Research*, **45**, W06426  
11  
12

13  
14 **Ashmore, P.E.** (1982) Laboratory modelling of gravel braided-stream morphology. *Earth*  
15 *Surface Processes and Landforms*, **7**, 201-225.  
16  
17

18  
19 **Ashmore, P.E.** (1991) How do gravel-bed rivers braid? *Canadian Journal of Earth Sciences*,  
20 **28**, 326-341.  
21  
22

23  
24 **Ashworth, P.J. and Lewin, J.** (2012) How do big rivers come to be different? *Earth-Science*  
25 *Reviews*, **114**, 84-107. doi 10.1016/j.earscirev.2012.05.003.  
26  
27

28  
29 **Ashworth, P.J., Sambrook Smith, G.H., Best, J.L., Bridge, J.S., Lane, S.N., Lunt, I.A.,**  
30 **Reesink, A.J.H., Simpson, C.J. and Thomas, R.E.** (2011) Evolution and sedimentology of a  
31 sandy braided channel fill and its differentiation from compound bar deposits. *Sedimentology*,  
32 **58**(7), 1860-1883. doi: 10.1111/j.1365-3091.2011.01242.x.  
33  
34  
35

36  
37 **Baas, J.H., Best, J.L., Peakall, J. and Wang, M.** (2009) A phase diagram for turbulent,  
38 transitional, and laminar clay suspension flows. *Journal of Sedimentary Research*, **79**, 162-183.  
39  
40

41  
42 **Baker, G.S., Jordan, T.E. and Pardy, J.** (2007) An introduction to Ground Penetrating Radar  
43 (GPR). In: *Stratigraphic analyses using GPR* - (Eds G.S. Baker and H.M. Jol), *GSA Special*  
44 *Publication*, **432**, 1-18.  
45  
46  
47

48  
49 **Best, J.L., Ashworth, P.J., Bristow, C.S. and Roden, J.E.** (2003) Three dimensional  
50 sedimentary architecture of a large, mid-channel sand braid bar, Jamuna River, Bangladesh.  
51 *Journal of Sedimentary Research*, **73**, 516-530.  
52  
53  
54  
55  
56  
57  
58  
59  
60

Draft paper: Variability in bar sedimentology in a large river, Version 6, 09/03/2011

1  
2 **Best, J.L., Ashworth, P.J., Sarker, M.H. and Roden, J.E.** (2007) The Brahmaputra-Jamuna  
3 River, Bangladesh. In: *Large Rivers; Geomorphology and Management* (Ed A. Gupta), John  
4 Wiley & Sons, Ltd, Chichester, pp. 395-430.

5  
6  
7  
8 **Blettler, M.C.M., Amsler, M.L., and Drago, I.E.** (2012) Hydraulic factors controlling the benthic  
9 invertebrate distribution within and among dunes of the Middle Parana River (Argentina) and  
10 sampling techniques. *Journal of South American Earth Sciences* **35**, 27-37.

11  
12  
13 **Blum, M., Martin, J., Milliken K. and Garvin M.** (2013) Paleovalley systems: Insights from  
14 Quaternary analogs and experiments. *Earth-Science Reviews*, **116**, pp. 128-169.

15  
16  
17  
18  
19 **Boersma, J.R.** (1967) Remarkable types of mega cross-stratification in the fluvial sequence  
20 of a subrecent distributary of the Rhine, Amerongen, The Netherlands. *Geologie en Mijnbouw*,  
21 **46**, 217-235.

22  
23  
24  
25  
26 **Bonetto, A.A. and Orfeo, O.O.** (1984) Caracteres sedimentologicos de la carga en  
27 suspension de Río Paraná entre Confluencia y Esquina (prov. de Corrientes, R.A.).  
28 *Mineralogía, Petrología, Sedimentología*, **15**, 51-61.

29  
30  
31  
32  
33 **Bridge, J.S.** (1993a) Description and interpretation of fluvial deposits – a critical perspective.  
34 *Sedimentology* **40**(4), 801-810.

35  
36  
37  
38  
39 **Bridge, J.S.** (1993b) The interaction between channel geometry, water flow, sediment transport  
40 and deposition in braided rivers. In: *Braided Rivers* (Eds J.L. Best and C.S. Bristow), *Geological*  
41 *Society Special Publication* **75**, pp. 13-71. London.

42  
43  
44  
45  
46 **Bridge, J.S.** (2003) Rivers and Floodplains; Forms, Processes, and Sedimentary Record.  
47 Blackwell Publishing, Oxford, 491 pp.

48  
49  
50  
51 **Bridge, J.S.** (2009) Advances in Fluvial Sedimentology using GPR. In: *Ground Penetrating*  
52 *Radar; Theory and Applications* (Ed H.M. Jol), Elsevier, 323-359.

53  
54  
55  
56  
57 **Bridge, J.S. and Lunt, I.A.** (2006) Depositional models of braided rivers. In: *Braided Rivers;*  
58 *Processes, Deposits, Ecology and Management* (Eds. G.H. Sambrook Smith, J.L. Best, C.S.

Draft paper: Variability in bar sedimentology in a large river, Version 6, 09/03/2011

1  
2 Bristow and G.E. Petts), International Association of Sedimentologists Special Publication, **36**,  
3  
4 11-50.

5  
6 **Bristow C. S.** (1987) Brahmaputra River: Channel migration and deposition, *Recent*  
7  
8 *Developments in Fluvial Sedimentology*, (Eds. Ethridge F. G., Flores R. M., Harvey M. D.)  
9  
10 Society of Economic Paleontologists and Mineralogists Special Publication, **39**, 63–74.

11  
12 **Bristow, C.S.** (1993) Sedimentary structures exposed in bar tops in the Brahmaputra River  
13  
14 Bangladesh. In *Braided Rivers* (Eds. Best, J.L. and Bristow, C.S. (Eds.) Geological Society of  
15  
16 London Special Publication, **75**, pp. 277-289.

17  
18 **Davidson, S.K., Leleu, S., and North, C.P.** (2011) *From river to rock record: the preservation*  
19  
20 *of fluvial sediments and their subsequent interpretation*. SEPM Special Publication 97, SEPM  
21  
22 (Society for Sedimentary Geology), pp. 3-5.

23  
24 **Drago, E.C. and Amsler, M.L.** (1998) Bed sediment characteristics in the Parana and  
25  
26 Paraguay rivers. *Water International*, **23**, 174-183.

27  
28 **Edmonds, D.A. and Slingerland, R.L.** (2010) Significant effect of sediment cohesion on delta  
29  
30 morphology. *Nature Geoscience*, **3**, 105-109.

31  
32 **Ethridge, F.G.** (2011) Interpretation of ancient fluvial channel deposits: review and  
33  
34 recommendations. *From River to Rock Record: the Preservation of Fluvial Sediments and their*  
35  
36 *Subsequent Interpretation*. (Eds. Davidson, S.K., Leleu, S., North, C.P.) *SEPM Special*  
37  
38 *Publication*, **97**, 9-35.

39  
40 **Federici, B. and Seminara, G.** (2006) Effect of suspended load on sandbar instability. *Water*  
41  
42 *Resources Research*, **42**.

43  
44 **Fielding, C.R.** (2007) Sedimentology and stratigraphy of large river deposits: Recognition in the  
45  
46 ancient record and distinction from 'incised valley fills'. In: *Large Rivers; Geomorphology and*  
47  
48 *Management* (Ed A. Gupta), pp. 97-113. Wiley, Chichester.

Draft paper: Variability in bar sedimentology in a large river, Version 6, 09/03/2011

- 1  
2 **Fielding C.R., Ashworth P.J., Best J.L., Prokocki E.W. Sambrook Smith G.H.** (2012)  
3  
4 Tributary, distributary and other fluvial patterns: What really represents the norm in the  
5  
6 continental rock record? *Sedimentary Geology*, **261-262**, 15-32.  
7
- 8 **Frings, R.M.** (2008) Downstream fining in large sand-bed rivers. *Earth-Science Reviews*, **87**,  
9  
10 39-60.  
11
- 12 **Gupta, A.** (2007) Large Rivers; Geomorphology and Management. John Wiley and Sons.  
13
- 14 **Haszeldine, R.S.** (1982) Descending tabular cross-bed sets and bounding surfaces from a  
15  
16 fluvial channel in the Upper Carboniferous of North-East England. *Journal of Sedimentary*  
17  
18 *Petrology*, **53**, 1233–1247.  
19
- 20 **Hickin, E.J.** (1993) Fluvial facies models—a review of Canadian research: Progress in Physical  
21  
22 Geography, **17**, 205–222.  
23
- 24 **Horn, J.D., Joeckel, R.M. and Fielding, C.R.** (2012a) Progressive abandonment and planform  
25  
26 changes of the central Platte River in Nebraska, central USA, over historical timeframes.  
27  
28 *Geomorphology*, **139–140**, 372–383;  
29
- 30 **Horn, J.D., Fielding, C.R., Joeckel, R.M.** (2012b) Revision of the Platte River alluvial facies  
31  
32 model through observation of extant channels and barforms, and subsurface alluvial valley fills.  
33  
34 *Journal of Sedimentary Research*, **82(2)**, 72-91.  
35
- 36 **Hovius, N. and Leeder, M.** (1998) Clastic sediment supply to basins. *Basin Research*, **10**, 1-5.  
37
- 38 **Jopling, A.V.** (1965) Laboratory study of the distribution of grain sizes in cross bedded  
39  
40 deposits. In: *Primary Sedimentary Structures and Their Hydrodynamic Interpretation* (Ed.  
41  
42 Middleton, G.V) *SEPM Special Publication*, **12**. 53–65.  
43  
44
- 45 **Kostaschuk, R., Shugar, D., Best, J., Parsons, D., Lane, S., Hardy, R. and Orfeo, O.** (2009)  
46  
47 Suspended sediment transport and deposition over a dune: Río Parana, Argentina. *Earth*  
48  
49 *Surface Processes and Landforms*, **34**, 1605-1611.  
50  
51  
52  
53  
54  
55  
56  
57  
58  
59  
60

Draft paper: Variability in bar sedimentology in a large river, Version 6, 09/03/2011

- 1  
2 **Lane, S.N., Parsons, D.R., Best, J.L., Orfeo, O., Kostaschuk, R.A. and Hardy, R.J.** (2008)  
3  
4 Causes of rapid mixing at a junction of two large rivers: Río Parana and Río Paraguay,  
5  
6 Argentina. *Journal of Geophysical Research-Earth Surface*, **113**.  
7  
8 **Larue, D.K. and Hovadik, J.** (2006) Connectivity of channelized reservoirs: a modelling  
9  
10 approach. *Petroleum Geoscience*, **12**, 291-308.  
11  
12 **Latrubesse, E.M.** (2008) Patterns of anabranching channels: The ultimate end-member  
13  
14 adjustment of mega rivers. *Geomorphology*, **101**, 130-145.  
15  
16 **Latrubesse, E.M. and Franzinelli, E.** (2005) The late Quaternary evolution of the Negro River,  
17  
18 Amazon, Brazil: implications for island and floodplain formation in large anabranching tropical  
19  
20 systems. *Geomorphology*, **70**, 372-397.  
21  
22 **Leclair, S. F. and Bridge, J. S.** (2001) Quantitative interpretation of sedimentary structures  
23  
24 formed by river dunes. *Journal of Sedimentary Research*, **71**(5), 713-716.  
25  
26 **Lunt, I.A. and Bridge, J.S.** (2004) Evolution and deposits of a gravelly braid bar, Sagavanirktok  
27  
28 River, Alaska. *Sedimentology*, **51**, 415-432.  
29  
30 **Lunt, I.A., Bridge, J.S. and Tye, R.S.** (2004) A quantitative, three-dimensional depositional  
31  
32 model of gravelly braided rivers. *Sedimentology*, **51**, 377-414.  
33  
34 **Lynds, R. and Hajek, E.** (2006) Conceptual model for predicting mudstone dimensions in  
35  
36 sandy braided-river reservoirs. *AAPG Bulletin*, **90**, 1273-1288.  
37  
38 **Martinius, A.W. and Van den Berg, J.H.** (2010) Atlas of sedimentary structures in estuarine  
39  
40 and tidally-influenced river deposits of the Rhine-Meuse-Scheldt system; Their application to the  
41  
42 interpretation of analogous outcrop and subsurface depositional systems. EAGE Publications,  
43  
44 Houten, 298 pp.  
45  
46 **Miall, A.D.** (2006) How do we identify big rivers? And how big is big? *Sedimentary Geology*,  
47  
48 **186**, 39-50.  
49  
50  
51  
52  
53  
54  
55  
56  
57  
58  
59  
60



Draft paper: Variability in bar sedimentology in a large river, Version 6, 09/03/2011

1  
2 **Miall, A.D.** (1996) The geology of fluvial deposits: sedimentary facies, basin analysis and  
3  
4 petroleum geology. Springer-Verlag, Berlin, 589 p.

5  
6 **Miall, A.D. and Jones, B.G.** (2003) Fluvial architecture of the Hawkesbury Sandstone  
7  
8 (Triassic), near Sydney, Australia. *Journal of Sedimentary Research*, **73**, 531-545.

9  
10 **Milliman, J.D. and Meade, R.H.** (1983) World-wide delivery of sediment to the oceans. *Journal*  
11  
12 *of Geology*, **91**, 1-21.

13  
14 **Nanson, G.C. and Knighton, A.D.** (1996) Anabranching rivers: Their cause, character and  
15  
16 classification. *Earth Surface Processes and Landforms*, **21**, 217-239.

17  
18 **Neal, A.** (2004) Ground-penetrating radar and its use in sedimentology: principles, problems  
19  
20 and progress. *Earth-Science Reviews*, **66**, 261-330.

21  
22 **Nicholas, A.P., Sandbach, S.D., Ashworth, P.J., Amsler, M.L., Best, J.L., Hardy, R.J., Lane,**  
23  
24 **S.N., Orfeo, O., Parsons, D.R., Reesink, A.J.H., Sambrook Smith, G.H., and Szupiany, R.N.**  
25  
26 (2012) Modelling hydrodynamics in the Río Paraná, Argentina: an evaluation and inter-  
27  
28 comparison of reduced-complexity and physics based models applied to a large sand-bed river.  
29  
30 *Geomorphology*, **169-170**, 192-211.

31  
32 **Nicholas, A.P.** (2013) Morphodynamic diversity of the world's largest rivers. *Geology* **41**(4) 475-  
33  
34 478.

35  
36 **Orfeo, O. and Steveaux, J.** (2002) Hydraulic and morphological characteristics of middle and  
37  
38 upper reaches of the Parana River (Argentina and Brazil). *Geomorphology*, **44**, 309-322.

39  
40 **Paoli, C., Iriondo, M. and García, N.** (2010) Características de las cuencas de aporte. In: El  
41  
42 Río Paraná en su trama medio. *Contribución al conocimiento y prácticas ingenieriles en un*  
43  
44 *grande río llanura* (Eds C. Paoli and M.I. Schreider), 1. Centro Publicaciones, Universidad  
45  
46 Nacional de Littoral, Santa Fé.

47  
48 **Parker, N.O., Sambrook Smith, G.H., Ashworth, P.J., Best, J.L., Lane, S.N., Lunt, I.A.,**  
49  
50 **Simpson, C.J., Thomas, R.E.**(2013) Quantification of the relation between surface  
51  
52

Draft paper: Variability in bar sedimentology in a large river, Version 6, 09/03/2011

morphodynamics and subsurface sedimentological product in sandy braided rivers.

*Sedimentology* **60**(3), 820-839

**Parsons, D.R., Amsler, M.L., Szupiany, R.N., Ashworth, P.J., Best, J.L., Hardy, R.J., Lane, S.N., Nicholas, A.P., Orfeo, O.O., Sambrook Smith, G.H., Reesink, A.J.H. and Sandbach, S.D.** (2009) Process-product relationships in a large river: the Río Paraná, Argentina. In: *River, Coastal and Estuarine Morphodynamics* (Eds C.A. Vionnet, M.H. García, E.M. Latrubesse and G.M.E. Perillo), **1**, pp. 51-56. Taylor & Francis Group, London, Santa Fé.

**Parsons, D.R., Best, J.L., Lane, S.N., Orfeo, O., Hardy, R.J. and Kostaschuk, R.** (2007) Form roughness and the absence of secondary flow in a large confluence-diffuence, Río Parana, Argentina. *Earth Surface Processes and Landforms*, **32**, 155-162.

**Parsons, D.R., Best, J.L., Orfeo, O., Hardy, R.J., Kostaschuk, R. and Lane, S.N.** (2005) Morphology and flow fields of three-dimensional dunes, Río Parana, Argentina: Results from simultaneous multibeam echo sounding and acoustic Doppler current profiling. *Journal of Geophysical Research-Earth Surface*, **110**.

**Potter, P.E.** (1978) Significance and origin of big rivers. *Journal of Geology*, **86**, 13-33.

**Ramonell, C.G., Amsler, M.L. and Toniolo, H.A.** (2002) Shifting modes of the Paraná River thalweg in its middle-lower reaches. *Zeitschrift für Geomorphologie*, Supl Bd, 129-142.

**Reesink, A.J.H. and Bridge, J.S.** (2007) Influence of superimposed bedforms and flow unsteadiness on formation of cross strata in dunes and unit bars. *Sedimentary Geology*, **202**, 281-296.

**Reesink, A.J.H. and Bridge, J.S.** (2009) Influence of bedform superimposition and flow unsteadiness on the formation of cross strata in dunes and unit bars - Part 2, further experiments. *Sedimentary Geology*, **222**, 274-300.

Draft paper: Variability in bar sedimentology in a large river, Version 6, 09/03/2011

1  
2 **Reesink, A.J.H. and Bridge, J.S.** (2011) Evidence of bedform superimposition and flow  
3 unsteadiness in unit-bar deposits, South Saskatchewan River, Canada. *Journal of Sedimentary*  
4 *Research*, **81**(11), 814-840.  
5  
6  
7

8 **Rozo, M.G., Nogueira, A.C.R. and Truckenbrodt, W.** (2012) The anastomosing pattern and  
9 the extensively distributed scroll bars in the middle Amazon River. *Earth Surface Processes and*  
10 *Landforms*, **37**(14), 1471–1488  
11  
12  
13

14 **Sambrook Smith, G.H., Ashworth, P.J., Best, J.L., Woodward, J. and Simpson, C.J.** (2006)  
15 The sedimentology and alluvial architecture of the sandy braided South Saskatchewan River,  
16 Canada. *Sedimentology*, **53**, 413-434.  
17  
18  
19  
20

21 **Sambrook Smith, G.H., Ashworth, P.J., Best, J.L., Lunt, I.A., Orfeo, O. and Parsons, D.R.**  
22 (2009) The sedimentology and alluvial architecture of a large braid bar, Río Paraná, Argentina.  
23 *Journal of Sedimentary Research*, **79**, 629-642.  
24  
25  
26  
27

28 **Sambrook Smith, G.H., Best, J.L., Orfeo, O., Vardy, M.E. and Zinger, J.A.** (2013) Decimeter-  
29 scale in situ mapping of modern cross-bedded dune deposits using parametric echo sounding  
30 (PES): a new method for linking river processes and their deposits. *Geophysical Research*  
31 *Letters*, DOI: 10.1002/grl.50703.  
32  
33  
34  
35  
36

37 **Sandbach, S.D., Hardy, R.J., Lane, S.N., Parsons, D.R., Best, J.L., Ashworth, P.J.,**  
38 **Reesink, A.J.H., Amsler, M.L., Szupiany, R.N., Nicholas, A.P., Orfeo, O. and Sambrook**  
39 **Smith, G.H.** (2010) Three-dimensional modelling of a very large river; the Río Paraná. In:  
40 *Proceedings of the IAHR River Flow Conference*. Bundesanstalt fuer Wasserbau, pp. 409-417.  
41  
42  
43  
44

45 **Sandbach, S.D., Lane, S.N., Hardy, Amsler, M.L., Ashworth, P.J., Best, J.L., R.J., Nicholas,**  
46 **A.P., Orfeo, O., Parsons, D.R., Reesink, A.J.H., Sambrook Smith, G.H. and Szupiany, R.N.**  
47 (2012) Application of a roughness-length representation to parameterize energy loss in 3-D  
48 numerical simulations of large rivers, *Water Resources Research*, **48**, W12501,  
49 doi:10.1029/2011WR011284  
50  
51  
52  
53  
54  
55  
56  
57  
58  
59  
60

Draft paper: Variability in bar sedimentology in a large river, Version 6, 09/03/2011

1  
2 **Santos, M.L. and Steveaux, J.C.** (2000) Facies and architectural analysis of channel sandy  
3 macroforms in the Upper Paraná River. *Quaternary International*, **72**, 87-94.

4  
5  
6 **Schumm, S.A. and Winkley, B.R.** (1994) The character of large alluvial rivers. In: *The*  
7 *character of large alluvial rivers* (Eds S.A. Schumm and B.R. Winkley), American Society of Civil  
8 Engineers. 1-9.

9  
10  
11 **Sheriff, R.E. and Geldart, L.P.** (1982) Exploration seismology, Volume 1: history, theory and  
12 data acquisition, Cambridge University Press, Cambridge, UK.

13  
14  
15 **Shugar, D.H., Kostaschuk, R., Best, J.L., Parsons, D.R., Lane, S.N., Orfeo, O. and Hardy,**  
16 **R.J.** (2010) On the relationship between flow and suspended sediment transport over the crest  
17 of a sand dune, Río Parana, Argentina. *Sedimentology*, **57**, 252-272.

18  
19  
20 **Singh, M., Singh, I.B. and Muller, G.** (2007) Sediment characteristics and transportation  
21 dynamics of the Ganga River. *Geomorphology*, **86**, 144-175.

22  
23  
24 **Skelly, R.L., Bristow, C.S. and Ethridge, F.G.** (2003) Architecture of channel-belt deposits in  
25 an aggrading shallow sandbed braided river: the lower Niobrara River, northeast Nebraska.  
26 *Sedimentary Geology*, **158**, 249-270.

27  
28  
29 **Smith, D.G. and Smith, N.D.** (1980) Sedimentation in anastomosed river systems: examples  
30 from alluvial valleys near Banff, Alberta. *Journal of Sedimentary Petrology*, **50**, 157-164.

31  
32  
33 **Smith, N.D.** (1974) Sedimentology and bar formation in the upper Kicking Horse River: A  
34 braided outwash stream. *Journal of Geology*, **82**, 205-223.

35  
36  
37 **Steveaux, J.C.** (1994) The upper Paraná River (Brazil): Geomorphology, sedimentation and  
38 palaeoclimatology. *Quaternary International*, **21**, 143-161.

39  
40  
41 **Szupiany, R.N., Amsler, M.L., Parsons, D.R. and Best, J.L.** (2009) Morphology, flow  
42 structure, and suspended bed sediment transport at two large braid-bar confluences. *Water*  
43 *Resources Research*, **45**, W05415, 19 PP.

Draft paper: Variability in bar sedimentology in a large river, Version 6, 09/03/2011

1  
2 **Van de Meene, E.A., Van der Staaij, J. and Hock, T.L.** (1979) The Van der Staaij suction  
3  
4 corer - a simple apparatus for drilling below the ground water table. Rijks Geologische Dienst,  
5  
6 Haarlem 1-15.  
7

8  
9 **Van den Berg, J.H. and Van Gelder, A.** (1993) A new bedform stability diagram, with  
10  
11 emphasis on the transition of ripples to plane bed in flows over fine sand and silt. In: *Alluvial*  
12  
13 *Sedimentation* (Eds M. Marzo and C. Puidefabregas) *International Association of*  
14  
15 *Sedimentologists Special Publication*, **17**, Blackwell Scientific Publications, Oxford.  
16

17  
18 **Valente, C.R. and Latrubesse, E.M.** (2012) Fluvial archive of peculiar avulsive fluvial patterns  
19  
20 in the largest Quaternary intracratonic basin of tropical South America: The Bananal Basin,  
21  
22 Central-Brazil. *Palaeogeography, Palaeoclimatology, Palaeoecology* **356–357**, 62–74.  
23

24  
25 **Wunderlich, J. and Müller, S.** (2003) High-resolution sub-bottom profiling using parametric  
26  
27 acoustics. *International Ocean Systems*, **7**, 6-11.  
28  
29  
30  
31  
32

### 33 **FIGURE CAPTIONS**

34  
35 **Fig. 1.** Location of A) the study site, B) the two study reaches and the study bars within the  
36  
37 reach that are located near C) the Río Paraguay- Río Paraná confluence and D) near Santa Fe.  
38  
39

40  
41  
42 **Fig. 2.** Oblique aerial views of the bars investigated herein also showing the GPR survey lines  
43  
44 and core locations. Arrows indicate flow direction. More details are given in Table 1.  
45  
46

47  
48  
49 **Fig. 3.** GPR profiles with facies interpretations: examples from U1 (A,B), U2 (C), U3 (D), U4 (E),  
50  
51 U5 (F), C2 (G) and C3 (H). Labels: [I] horizontal transition between facies 1A and 1B. [II], [III]  
52  
53 and [IV] are facies 2 with chaotic, discontinuous, and trough-shaped geometries of the  
54  
55  
56  
57  
58  
59  
60

Draft paper: Variability in bar sedimentology in a large river, Version 6, 09/03/2011

1  
2 reflections, and [V] are complete dune profiles. Colours in (H) are facies interpretations: red is  
3  
4 facies 1A, yellow is facies 1B, green is facies 2, and blue lines are facies 3.  
5  
6  
7

8  
9 **Fig. 4.** Maps of spatial averages of GPR facies percentages (vertical sum of a single facies  
10 divided by the vertical sum of all facies within 200 x 200 m windows shifted in 20 m increments)  
11 for bars where GPR surveys were undertaken. See text for explanation of labels A-O.  
12  
13  
14

15  
16  
17 **Fig 5.** Core logs from the bars investigated herein: (A) bar head of U1, (B) left wing of U1, (C)  
18 bar head of U2, (D) right bar tail of U2, (E) U3, (F) bar head of U5 and (G) bar tail of C2. Also  
19 shown are associated photos from each of the cores (H-N).  
20  
21  
22  
23  
24  
25

26 **Fig. 6.** Landsat images (Bands 1, 2 and 3) showing the temporal development of bars in area U  
27 . Note that the flow discharge varies between images but most images are at low flow.  
28  
29  
30  
31  
32

33 **Fig. 7.** Along-stream and cross-stream GPR profiles and interpretation of the geometry of the  
34 bounding surfaces in U1 (A-D), U2 (E-H), U5 (I-L) and C2 (M-P).  
35  
36  
37  
38

39 **Fig. 8.** GPR fence-plot and cores of U3 (Fig. 2E) showing an internal composition of a small and  
40 new bar that is dominated by large-scale cross-strata (facies 1A).  
41  
42  
43  
44  
45

46 **Fig. 9.** Matrix of distributions of the percentage of facies within the bars (vertical proportion).  
47 Means and standard deviations are given per graph and visualized by stars with error bars. The  
48 percentages of the investigated surface-area where the facies are found are given in the pie-  
49 charts (with values).  
50  
51  
52  
53  
54  
55  
56  
57  
58  
59  
60

Draft paper: Variability in bar sedimentology in a large river, Version 6, 09/03/2011

1  
2 **Fig 10.** A) Trench from bar D3 showing interbedded dune sets, ripple co-sets and clay layers.  
3  
4 B) Trench from bar D2 showing angle-of-repose unit-bar sets. Note the contrast in grain-size  
5  
6 sorting in the cross-strata when compared with that from further upstream (see Fig. 5H). C)  
7  
8 Cutbank from bar D1. Note the locally deformed cross-strata at the base of the exposure and  
9  
10 also the fine-grained horizon that extended over hundreds of metres. D) Core log from bar D1.  
11  
12 E) Core log from bar D2. F) Core log from bar D2. See Fig. 2 for locations of trenches and  
13  
14 cores.  
15  
16  
17  
18  
19

20 **Fig. 11:** A) Parametric Echo Sounder (PES) profile showing channel bed surface morphology  
21  
22 and subsurface architecture from the channel adjacent to C1. PES reflection surfaces reveal: i)  
23  
24 reactivation surfaces within dunes and deposits characterised by sets composed of (C, $\alpha$ ) high-  
25  
26 angle, relatively straight, low-amplitude reflections: these are interpreted as angle-of-repose  
27  
28 cross strata formed by dunes; and ii) co-sets (C, $\beta$ ) composed of lower-angle, higher-amplitude  
29  
30 internal reflections with less regular geometries: these are interpreted as stacks of inclined  
31  
32 cross-stratified sets formed by dunes migrating down the reduced lee slope of a larger host  
33  
34 dune or bar.  
35  
36  
37  
38  
39  
40  
41  
42  
43  
44  
45  
46  
47  
48  
49  
50  
51  
52  
53  
54  
55  
56  
57  
58  
59  
60

1  
2  
3  
4  
5  
6  
7  
8  
9  
10  
11  
12  
13  
14  
15  
16  
17  
18  
19  
20  
21  
22  
23  
24  
25  
26  
27  
28  
29  
30  
31  
32  
33  
34  
35  
36  
37  
38  
39  
40  
41  
42  
43  
44  
45  
46  
47  
48  
49  
50  
51  
52  
53  
54  
55  
56  
57  
58  
59  
60

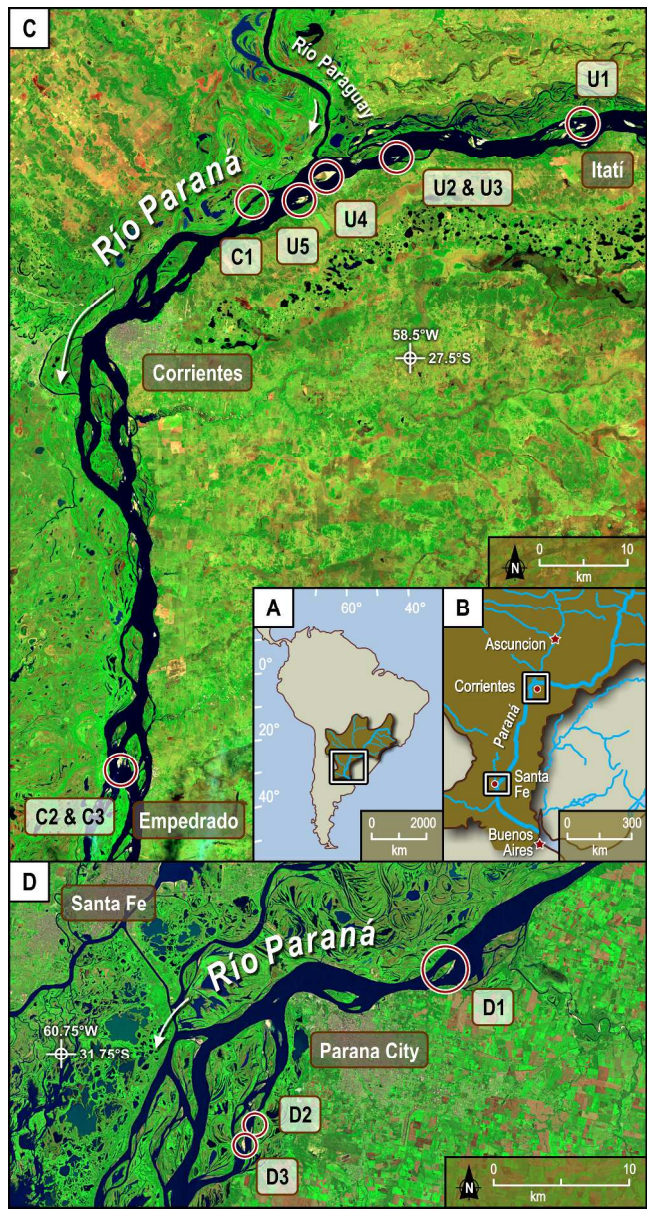


Fig. 1. Location of A) the study site, B) the two study reaches and the study bars within the reach that are located near C) the Río Paraguay- Río Paraná confluence and D) near Santa Fe.  
210x395mm (300 x 300 DPI)



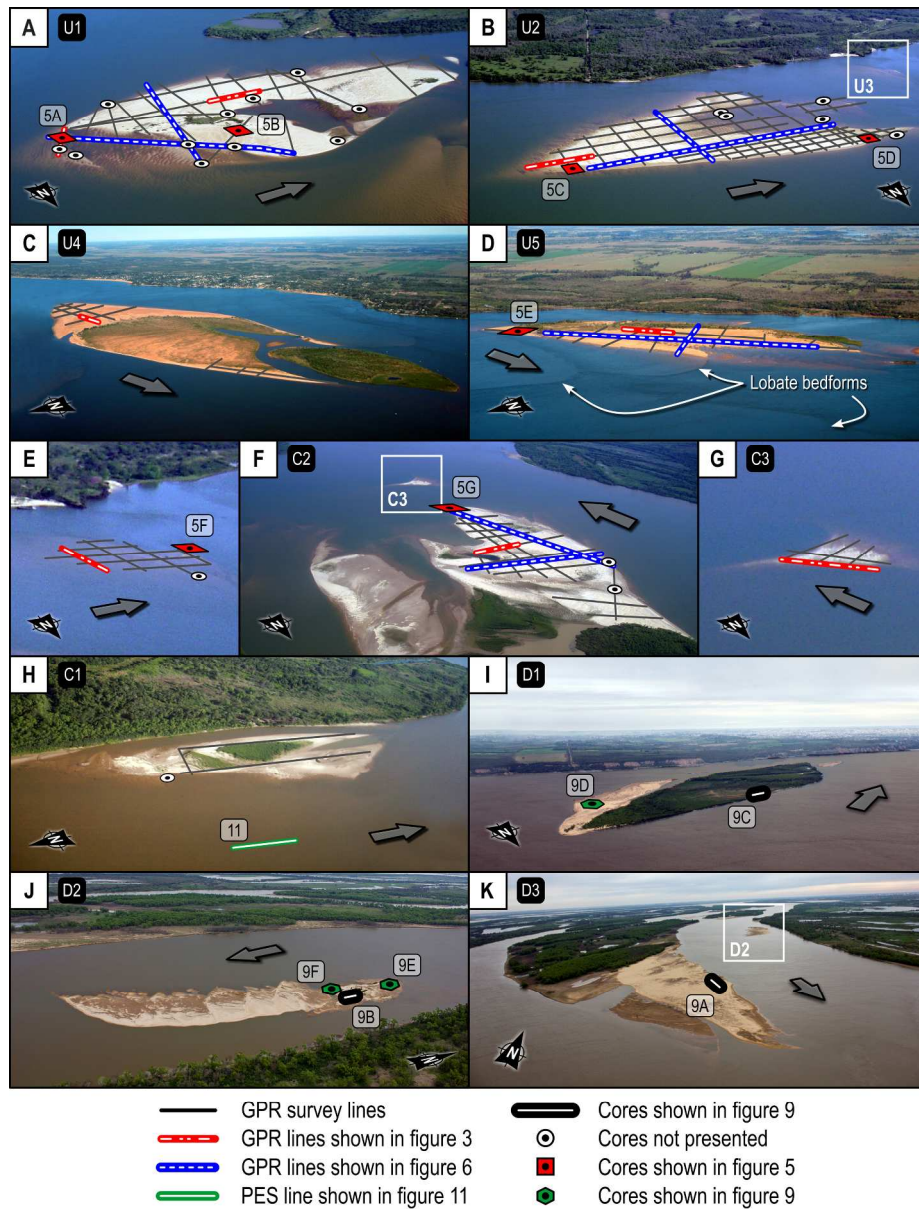


Fig. 2. Oblique aerial views of the bars investigated herein also showing the GPR survey lines and core locations. Arrows indicate flow direction. More details are given in Table 1.  
222x290mm (300 x 300 DPI)

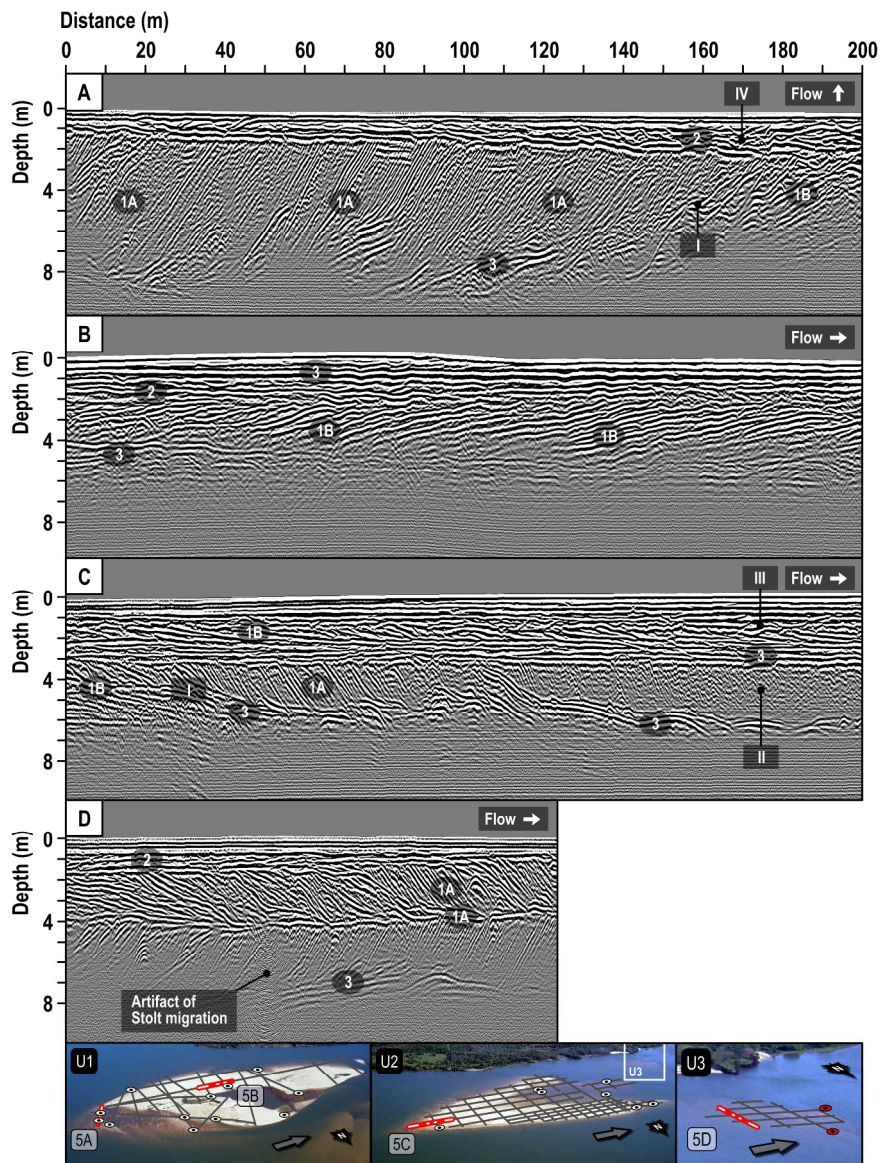


Fig. 3. GPR profiles with facies interpretations: examples from U1 (A,B), U2 (C), U3 (D), U4 (E), U5 (F), C2 (G) and C3 (H). Labels: [I] horizontal transition between facies 1A and 1B. [II], [III] and [IV] are facies 2 with chaotic, discontinuous, and trough-shaped geometries of the reflections, and [V] are complete dune profiles. Colours in (H) are facies interpretations: red is facies 1A, yellow is facies 1B, green is facies 2, and blue lines are facies 3.  
 229x311mm (300 x 300 DPI)

1  
 2  
 3  
 4  
 5  
 6  
 7  
 8  
 9  
 10  
 11  
 12  
 13  
 14  
 15  
 16  
 17  
 18  
 19  
 20  
 21  
 22  
 23  
 24  
 25  
 26  
 27  
 28  
 29  
 30  
 31  
 32  
 33  
 34  
 35  
 36  
 37  
 38  
 39  
 40  
 41  
 42  
 43  
 44  
 45  
 46  
 47  
 48  
 49  
 50  
 51  
 52  
 53  
 54  
 55  
 56  
 57  
 58  
 59  
 60

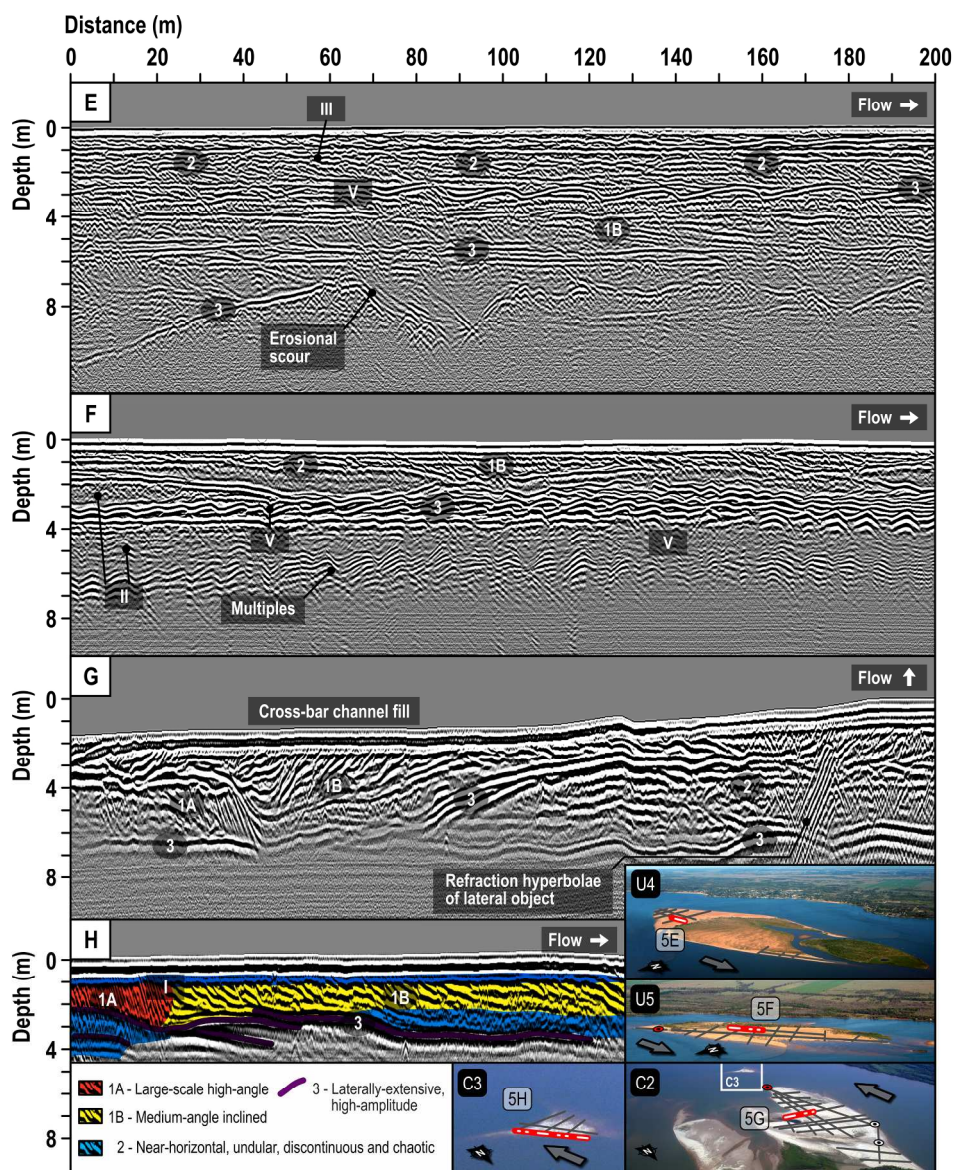


Fig. 3. GPR profiles with facies interpretations: examples from U1 (A,B), U2 (C), U3 (D), U4 (E), U5 (F), C2 (G) and C3 (H). Labels: [I] horizontal transition between facies 1A and 1B. [II], [III] and [IV] are facies 2 with chaotic, discontinuous, and trough-shaped geometries of the reflections, and [V] are complete dune profiles. Colours in (H) are facies interpretations: red is facies 1A, yellow is facies 1B, green is facies 2, and blue lines are facies 3.

211x264mm (300 x 300 DPI)

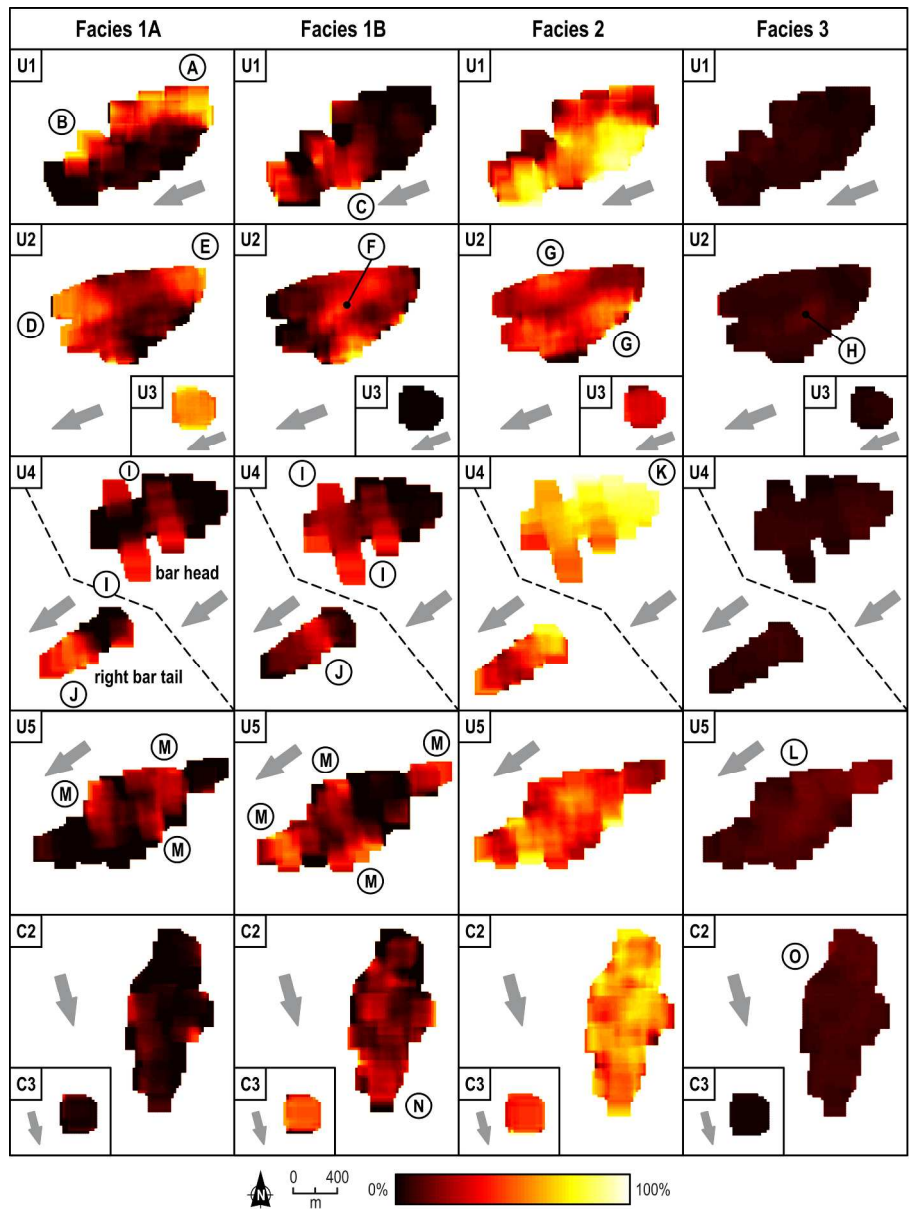


Fig. 4. Maps of spatial averages of GPR facies percentages (vertical sum of a single facies divided by the vertical sum of all facies within 200 x 200 m windows shifted in 20 m increments) for bars where GPR surveys were undertaken. See text for explanation of labels A-O.  
226x302mm (300 x 300 DPI)



1  
2  
3  
4  
5  
6  
7  
8  
9  
10  
11  
12  
13  
14  
15  
16  
17  
18  
19  
20  
21  
22  
23  
24  
25  
26  
27  
28  
29  
30  
31  
32  
33  
34  
35  
36  
37  
38  
39  
40  
41  
42  
43  
44  
45  
46  
47  
48  
49  
50  
51  
52  
53  
54  
55  
56  
57  
58  
59  
60

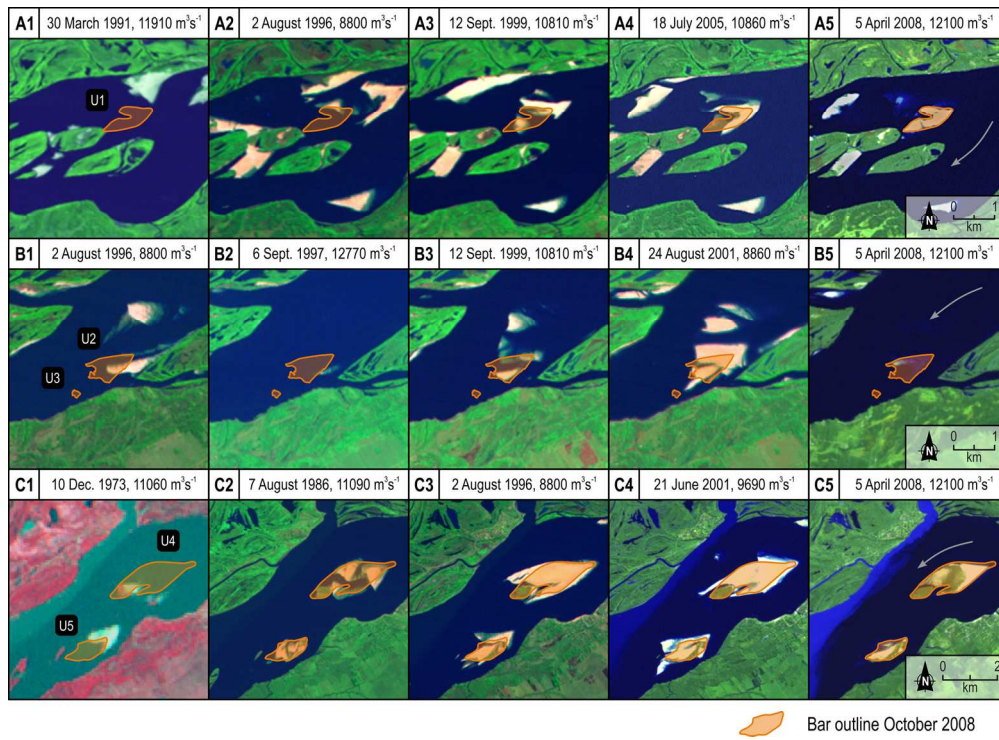
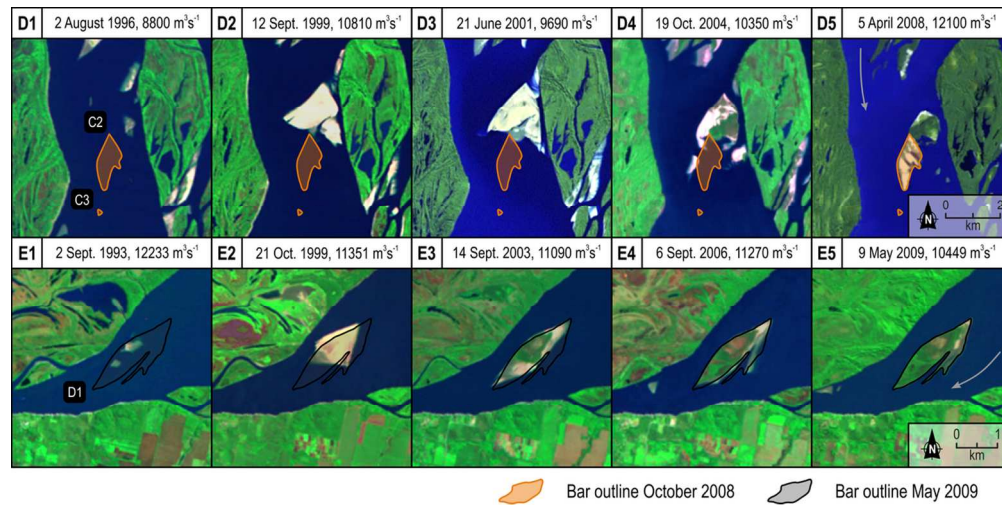


Fig. 6. Landsat images (Bands 1, 2 and 3) showing the temporal development of bars in area U. Note that the flow discharge varies between images but most images are at low flow.  
167x121mm (300 x 300 DPI)



24 Fig. 6. Landsat images (Bands 1, 2 and 3) showing the temporal development of bars in area U. Note that  
 25 the flow discharge varies between images but most images are at low flow.  
 26 114x56mm (300 x 300 DPI)

27  
28  
29  
30  
31  
32  
33  
34  
35  
36  
37  
38  
39  
40  
41  
42  
43  
44  
45  
46  
47  
48  
49  
50  
51  
52  
53  
54  
55  
56  
57  
58  
59  
60

1  
2  
3  
4  
5  
6  
7  
8  
9  
10  
11  
12  
13  
14  
15  
16  
17  
18  
19  
20  
21  
22  
23  
24  
25  
26  
27  
28  
29  
30  
31  
32  
33  
34  
35  
36  
37  
38  
39  
40  
41  
42  
43  
44  
45  
46  
47  
48  
49  
50  
51  
52  
53  
54  
55  
56  
57  
58  
59  
60

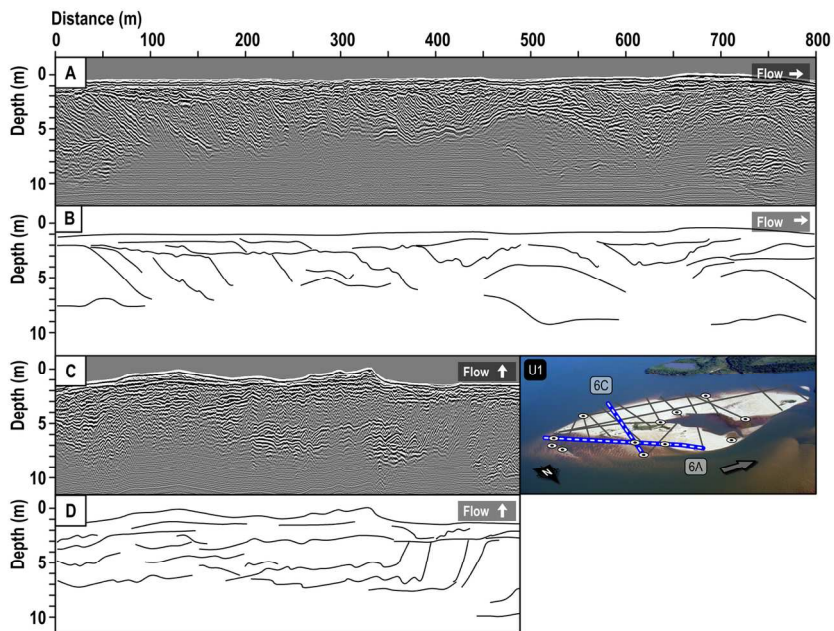


Fig. 7. Along-stream and cross-stream GPR profiles and interpretation of the geometry of the bounding surfaces in U1 (A-D), U2 (E-H), U5 (I-L) and C2 (M-P).  
151x99mm (300 x 300 DPI)



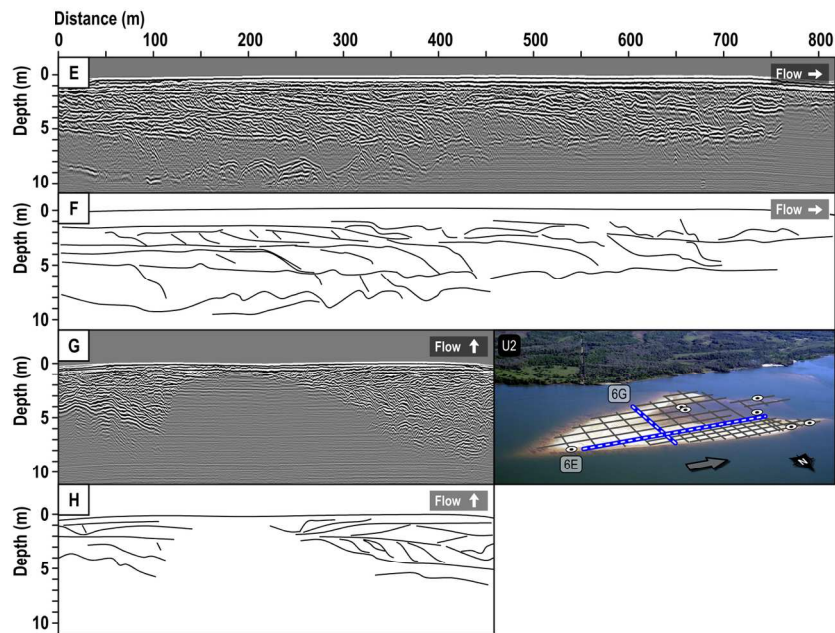


Fig. 7. Along-stream and cross-stream GPR profiles and interpretation of the geometry of the bounding surfaces in U1 (A-D), U2 (E-H), U5 (I-L) and C2 (M-P).  
151x99mm (300 x 300 DPI)

1  
2  
3  
4  
5  
6  
7  
8  
9  
10  
11  
12  
13  
14  
15  
16  
17  
18  
19  
20  
21  
22  
23  
24  
25  
26  
27  
28  
29  
30  
31  
32  
33  
34  
35  
36  
37  
38  
39  
40  
41  
42  
43  
44  
45  
46  
47  
48  
49  
50  
51  
52  
53  
54  
55  
56  
57  
58  
59  
60

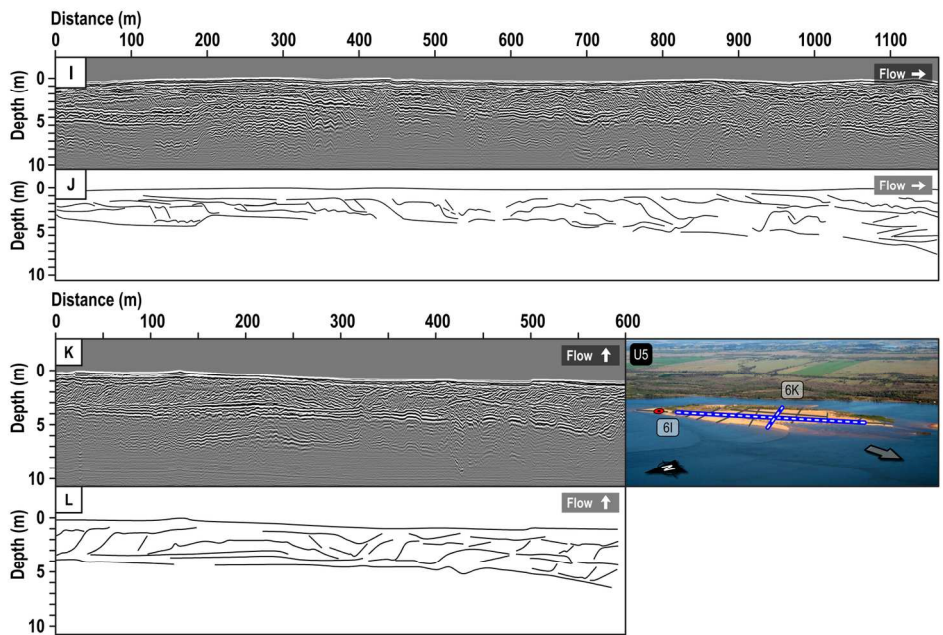


Fig. 7. Along-stream and cross-stream GPR profiles and interpretation of the geometry of the bounding surfaces in U1 (A-D), U2 (E-H), U5 (I-L) and C2 (M-P).  
151x99mm (300 x 300 DPI)

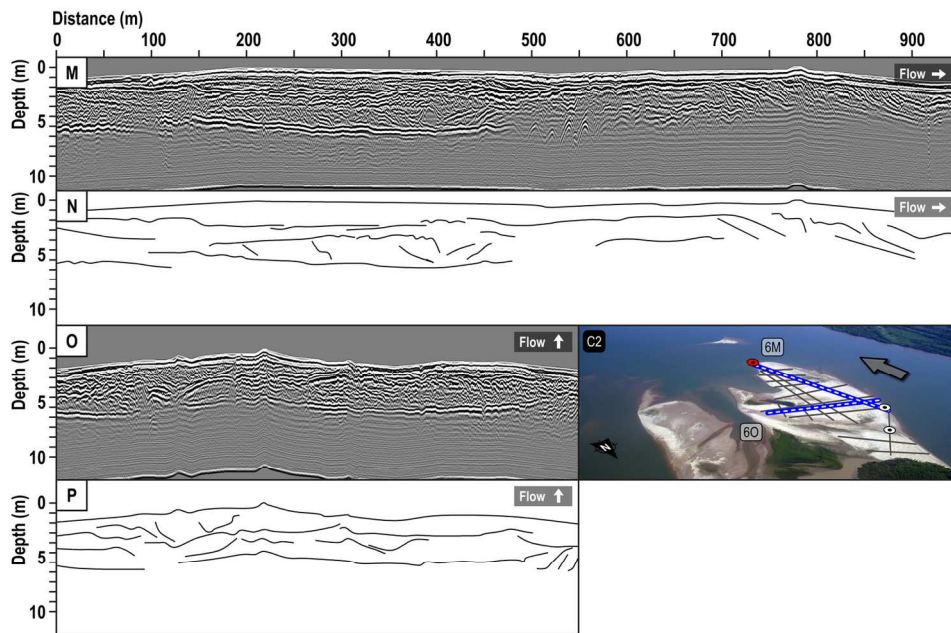


Fig. 7. Along-stream and cross-stream GPR profiles and interpretation of the geometry of the bounding surfaces in U1 (A-D), U2 (E-H), U5 (I-L) and C2 (M-P).  
151x99mm (300 x 300 DPI)

1  
2  
3  
4  
5  
6  
7  
8  
9  
10  
11  
12  
13  
14  
15  
16  
17  
18  
19  
20  
21  
22  
23  
24  
25  
26  
27  
28  
29  
30  
31  
32  
33  
34  
35  
36  
37  
38  
39  
40  
41  
42  
43  
44  
45  
46  
47  
48  
49  
50  
51  
52  
53  
54  
55  
56  
57  
58  
59  
60

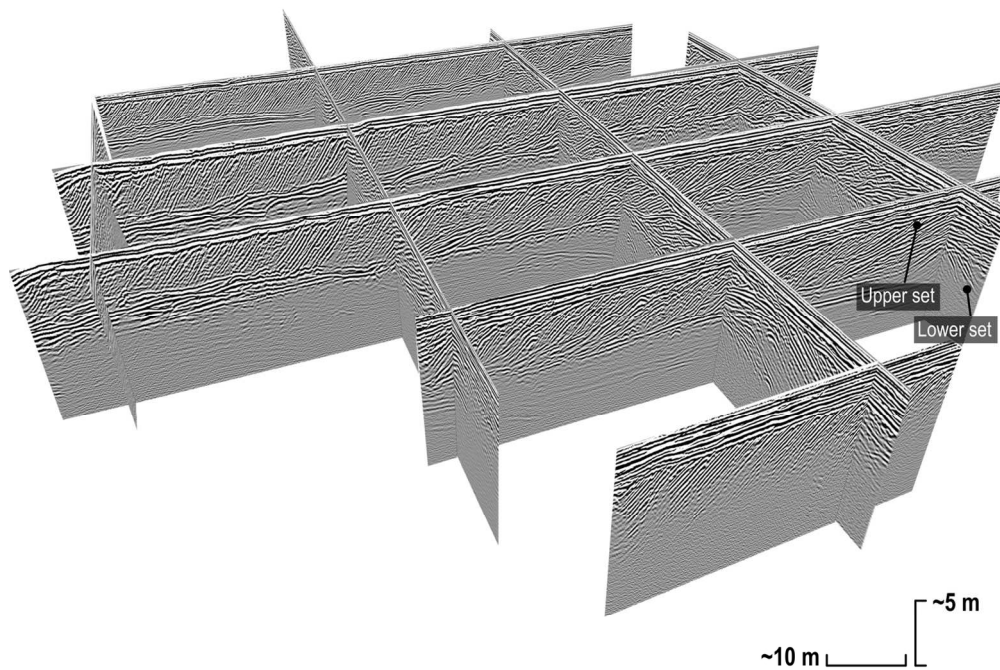


Fig. 8. GPR fence-plot and cores of U3 (Fig. 2E) showing an internal composition of a small and new bar that is dominated by large-scale cross-strata (facies 1A).  
135x108mm (300 x 300 DPI)

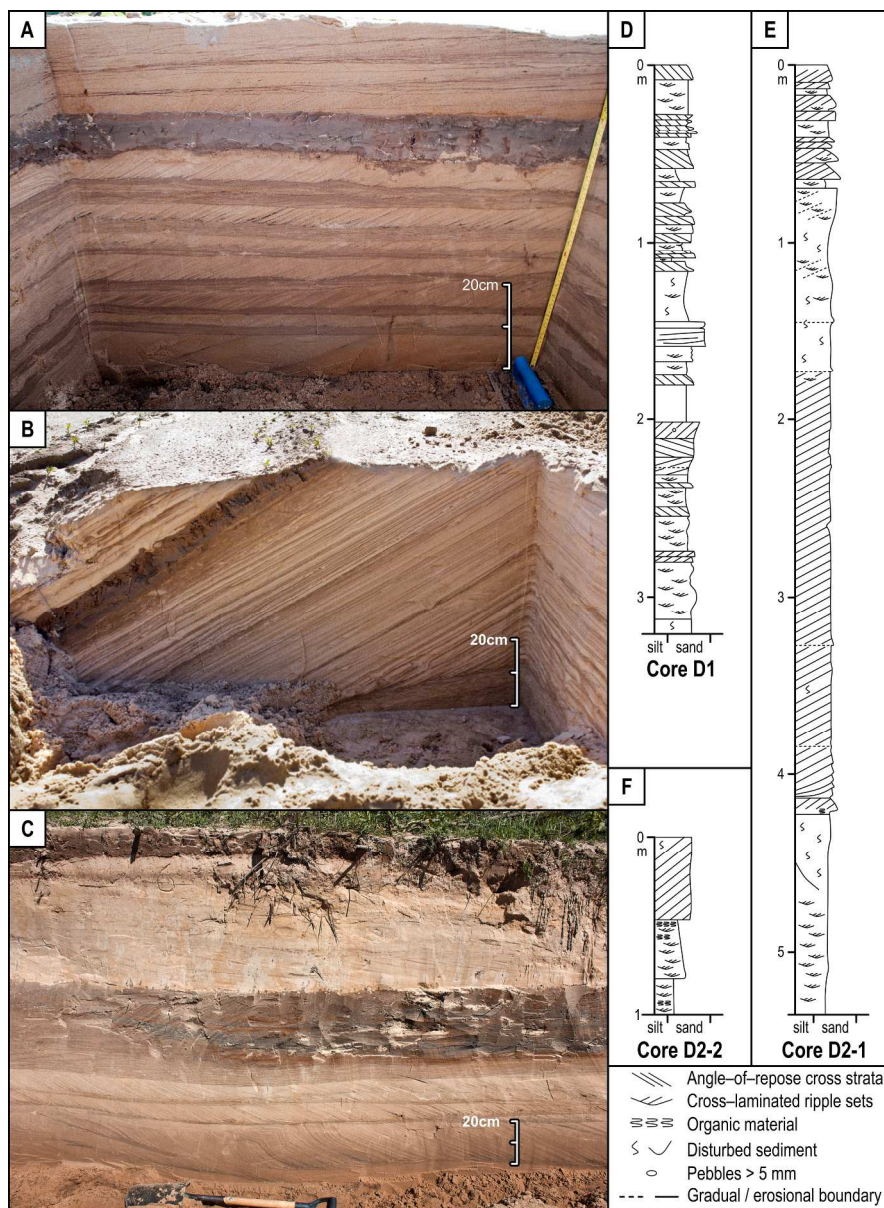


Fig 10. A) Trench from bar D3 showing interbedded dune sets, ripple co-sets and clay layers. B) Trench from bar D2 showing angle-of-repose unit-bar sets. Note the contrast in grain-size sorting in the cross-strata when compared with that from further upstream (see Fig. 5H). C) Cutbank from bar D1. Note the locally deformed cross-strata at the base of the exposure and also the fine-grained horizon that extended over hundreds of metres. D) Core log from bar D1. E) Core log from bar D2. F) Core log from bar D2. See Fig. 2 for locations of trenches and cores.

229x310mm (300 x 300 DPI)

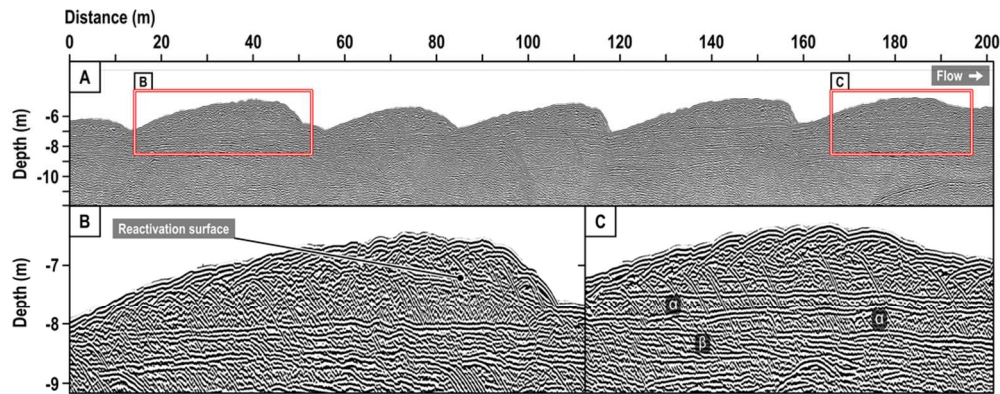


Fig. 11. A) Parametric Echo Sounder (PES) profile showing channel bed surface morphology and subsurface architecture from the channel adjacent to C1. PES reflection surfaces reveal: i) reactivation surfaces within dunes and deposits characterised by sets composed of (C,a) high-angle, relatively straight, low-amplitude reflections: these are interpreted as angle-of-repose cross strata formed by dunes; and ii) co-sets (C,B) composed of lower-angle, higher-amplitude internal reflections with less regular geometries: these are interpreted as stacks of inclined cross-stratified sets formed by dunes migrating down the reduced lee slope of a larger host dune or bar.

96x40mm (300 x 300 DPI)

**Table 1.** Background details of the investigated bars, their development observed in LandSat images, key observations from the GPR results, and sedimentary structures observed in cores.

Bar	Geomorphology & historical development (Figs 2 and 6)	Ground Penetrating Radar (Figs 3, 4, 7, 8)	Sedimentary structures in cores (Figs 5, 10)
<b>U1</b> <ul style="list-style-type: none"> <li>• 30 km upstream<sup>a</sup></li> <li>• ~6 years<sup>b</sup></li> <li>• 0.58 km<sup>2</sup> c</li> <li>• 8.3 km GPR</li> <li>• 13 cores</li> </ul>	<ul style="list-style-type: none"> <li>• Amalgamation in 1997 of two bars 0.5x0.3 and 0.3x1.7 km, approx. 1 km upstream is followed by migration of a bar front towards vegetated islands (Fig. 6 A1-3)</li> <li>• Stalling of the bar front just upstream of vegetated islands forms the current bar's right wing (Fig. 6 A3)</li> <li>• Gradual in-situ growth of the left bar wing causes enclosure and decrease in through-flow of water in the lee of the bar (Fig. 6 A3-5)</li> </ul>	<ul style="list-style-type: none"> <li>• Set of facies 1A with a thickness of ~8 m is present in the right wing (Figs. 3A, 7A-D), lateral extent of &gt;600 x &gt;300 m (Fig. 4 label A)</li> <li>• Downstream decrease in facies 1A thickness and increase of near-horizontal reflectors that can be traced to the inclined reflectors: association of the bar trough with the foresets (Fig. 7C-D)</li> <li>• The left wing contains a 4 m thick unit of upstream-dipping facies 1B (Fig. 3B) with a lateral extent of 550 x 200 m (Fig 4, label C) and associated with complete dune forms, facies 2</li> </ul>	<ul style="list-style-type: none"> <li>• The right wing is composed of a large set of angle-of-repose strata of which the base is not observed in the cores overlain by some small and medium-scale sets (Fig. 5A)</li> <li>• The left wing and bar centre are composed of thick units of ripple-sets with some medium-scale dune sets (Fig. 5B)</li> <li>• Trenches and cutbanks are dominated by dune deposits</li> </ul>
<b>U2</b> <ul style="list-style-type: none"> <li>• 8 km upstream<sup>a</sup></li> <li>• ~7 years<sup>b</sup></li> <li>• 0.43 km<sup>2</sup> c</li> <li>• 13.3 km GPR</li> <li>• 10 cores</li> </ul>	<ul style="list-style-type: none"> <li>• Developed from a 0.1 x 1 km, elongated bar that detached from the left bank in 1997 (Fig. 6B)</li> <li>• Coalesced with one or more unit bars migrating towards the left bank in 1999-2001, generating a winged shape</li> <li>• Continues to migrate downstream and develop its own elongated wings</li> </ul>	<ul style="list-style-type: none"> <li>• Large-scale sets of facies 1A lower in the bar head (Fig. 4 label E)</li> <li>• Stacking of units of facies 1A and 1B migrating to the bar centre from left and right (Fig. 7G-H)</li> <li>• Wings dominated by facies 1A (Fig 4. label D)</li> <li>• Facies 2 is dominant in the upper deposits and the bar flanks (Fig 4, label G)</li> <li>• Local abundance of facies 3 (Fig. 4 label H) likely an artefact of GPR attenuation in the bar centre (Fig. 7G)</li> </ul>	<ul style="list-style-type: none"> <li>• Cores from bar head and flanks characteristic contain a variety of ripple-co-sets and larger-scale sets associated with dunes and small unit bars</li> <li>• Distinct association of unit-bar forests with underlying fine-grained trough-deposits that include clay layers</li> </ul>
<b>U3</b> <ul style="list-style-type: none"> <li>• 7.5 km upstream<sup>a</sup></li> <li>• ~2 years<sup>b</sup></li> <li>• 0.025 km<sup>2</sup> c</li> <li>• 1.5 km GPR</li> <li>• 2 cores</li> </ul>	<ul style="list-style-type: none"> <li>• Initially attached to U2 during low flow (Fig. 6 B4)</li> <li>• Likely detached by a chute cut-off after 2001</li> </ul>	<ul style="list-style-type: none"> <li>• The internal structure is dominated (58%) by two amalgamated sets of facies 1A (Fig. 3D, Fig. 8)</li> </ul>	<ul style="list-style-type: none"> <li>• Cores composed of a large-scale set overlain by a few medium- and small-scale sets and underlain by fine-grained trough-deposits that include clay layers</li> </ul>
<b>U4*</b> <ul style="list-style-type: none"> <li>• 1 km<sup>a</sup> downstream</li> <li>• ~15 years<sup>b</sup></li> </ul>	<ul style="list-style-type: none"> <li>• Developed by amalgamation of bars in the period of 1977-1991 (Fig. 6 C1-2)</li> <li>• Remained in present location since mid 1970's</li> </ul>	<ul style="list-style-type: none"> <li>• Two sets of facies 1A and 1B in the bar head of 4 and 5 m thick respectively below 4-6 m of facies 2 (Fig. 4 label J)</li> <li>• Facies 1 dominates the bar tail (Fig. 4 label K)</li> </ul>	<ul style="list-style-type: none"> <li>• No cores</li> </ul>

<ul style="list-style-type: none"> <li>• 2.5 km<sup>2c</sup></li> <li>• 4.4 km GPR</li> <li>• no cores</li> </ul>	<ul style="list-style-type: none"> <li>• Dune forms common on flanks and bar head (Szupiany <i>et al.</i>, 2009)</li> <li>• Lateral accretion of large bedforms onto the bar develops its wings in 1995-96 and 2001 (Fig. 6 C3-4)</li> </ul>	<ul style="list-style-type: none"> <li>• Facies 2 dominant in the bar head and flanks</li> </ul>	
<p><b>U5</b></p> <ul style="list-style-type: none"> <li>• 4 km<sup>a</sup> downstream</li> <li>• ~27 years<sup>b</sup></li> <li>• 1.0 km<sup>2c</sup></li> <li>• 5.5 km GPR</li> <li>• 1 core</li> </ul>	<ul style="list-style-type: none"> <li>• Not reached by Río Paraguay sediment</li> <li>• Formed from symmetrical bar 1km upstream in 1973</li> <li>• Remained in present location since 1981</li> <li>• Characterised by amalgamation of unit bars – mosaic-like development (Fig. 6 C2-5)</li> </ul>	<ul style="list-style-type: none"> <li>• Data restricted to unvegetated right side</li> <li>• Facies 3 more abundant than other upstream bars (Fig. 4 label L), characteristically laterally extensive (Fig. 71-L), and dissecting the deposits into bar-scale units with typical sizes of 30-600 m</li> <li>• Facies 2 dominant</li> </ul>	<ul style="list-style-type: none"> <li>• Bottomsets of unit-bar deposits contain clay (Fig. 5M)</li> <li>• Large-scale unit (unit bar) composed internally of a mix of dune- and ripple-sets (Fig. 5F)</li> </ul>
<p><b>C1</b></p> <ul style="list-style-type: none"> <li>• 9 km<sup>a</sup> downstream</li> <li>• ~1 year<sup>b</sup></li> <li>• 0.085 km<sup>2c</sup></li> <li>• - km GPR</li> <li>• 1 core</li> </ul>	<ul style="list-style-type: none"> <li>• Developed in 2007 in a &lt;1km wide anabranch that is dominated by the silt-laden waters of the Río Paraguay (Fig. 2H)</li> <li>• Has remained in place since 2007, gradually elongated to ~1km</li> <li>• Bar surface dominated by silt</li> </ul>	<ul style="list-style-type: none"> <li>• GPR attempted, but radar signal was attenuated</li> </ul>	<ul style="list-style-type: none"> <li>• Unsuccessful coring attempts in too soft sediments</li> <li>• Retrieved core contained 36% ripple sets, 30% unidentifiable disturbed sediments, and cross-stratified sands</li> <li>• Abundant deformation observed in trench faces</li> </ul>
<p><b>C2</b></p> <ul style="list-style-type: none"> <li>• 73 km<sup>a</sup> downstream</li> <li>• ~4 years<sup>b</sup></li> <li>• 1.4 km<sup>2c</sup></li> <li>• 5.8 km GPR</li> <li>• 3 cores</li> </ul>	<ul style="list-style-type: none"> <li>• Located where Río Paraná and Río Paraguay are intermittently mixed (Fig. 1)</li> <li>• Bar head appeared in 1999, became vegetated in 2004 when the bar tail developed (Fig. 6D)</li> <li>• The present size of the bar tail was reached in 2007</li> </ul>	<ul style="list-style-type: none"> <li>• GPR on 1.3 x 0.7 km bar tail, part of a 2.0 x 1.0 km compound bar (Fig. 2F)</li> <li>• Facies 1A uncommon and restricted to small 10-100 m sets, facies 1B more common (Fig. 4 label N)</li> <li>• Facies 3 common and laterally extensive as in upstream bars (Fig. 4 label O; Fig. 7M-P)</li> </ul>	<ul style="list-style-type: none"> <li>• Cores show abundance of ripple sets (67%) and only one 0.5 m thick large-scale set (Fig. 5G,N) underlain by a thick ripple co-set</li> </ul>
<p><b>C3</b></p> <ul style="list-style-type: none"> <li>• 74 km<sup>a</sup> downstream</li> <li>• &lt;1 year<sup>b</sup></li> <li>• 0.025 km<sup>2c</sup></li> <li>• 0.5 km GPR</li> <li>• no cores</li> </ul>	<ul style="list-style-type: none"> <li>• Exposed during low flow in 2008</li> <li>• This incipient bar developed as an elevated part of a lobate lee slope that extends from the tail of C2 (Fig. 2G)</li> </ul>	<ul style="list-style-type: none"> <li>• Composed of a single large scale set that is dominated by facies 1B (Fig. 3H)</li> <li>• Underlain by a strong laterally extensive reflector below which no structures are observed</li> </ul>	<ul style="list-style-type: none"> <li>• No cores</li> </ul>

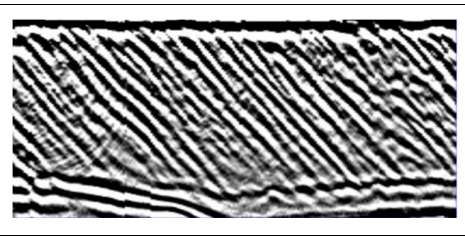
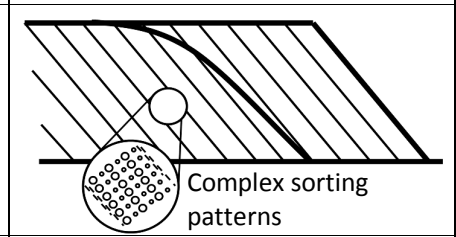
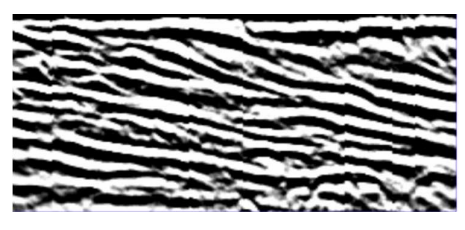
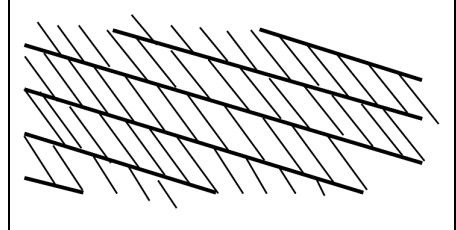
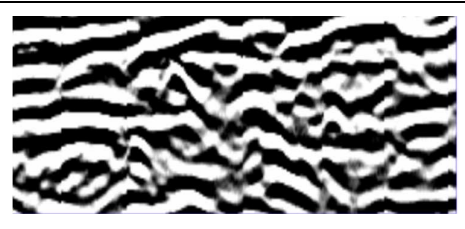
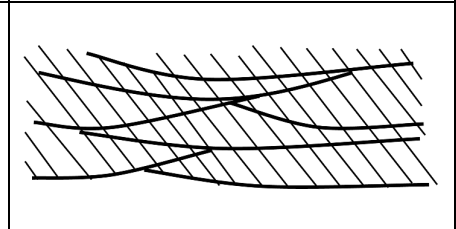
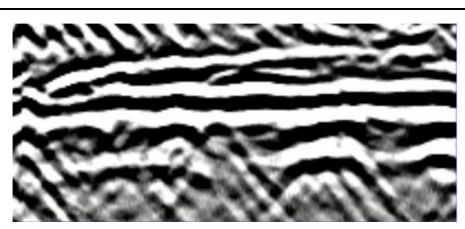
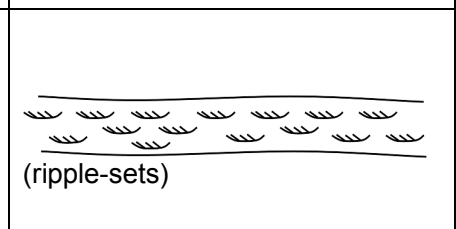


<p><b>D1</b></p> <ul style="list-style-type: none"> <li>• 520 km<sup>a</sup> downstream</li> <li>• &gt;38 years<sup>b</sup></li> <li>• 1.25 km<sup>2c</sup></li> <li>• - km GPR</li> <li>• 6 cores</li> </ul>	<ul style="list-style-type: none"> <li>• Located where waters of the Río Paraná and Río Paraguay are mixed</li> <li>• Submerged bars visible in early images, but first emerged in 1999 as a relatively short and wide bar and gradually became elongated</li> <li>• Vegetated from 2000 onwards (Fig. 6E)</li> <li>• Sandy parts restricted to bar head and left side</li> </ul>	<ul style="list-style-type: none"> <li>• GPR attempted, but radar signal was attenuated</li> </ul>	<ul style="list-style-type: none"> <li>• The 6 cores contained 46% ripples sets and 32% larger-scale sets but no bar-scale sets</li> <li>• Dune-sets were typically interbedded with finer-grained ripple sets (Fig. 10D)</li> <li>• Cut-banks on the right side contained more dune sets (Fig. 10C) and laterally-extensive clay layers and soil horizons of up to 0.4 m</li> </ul>
<p><b>D2</b></p> <ul style="list-style-type: none"> <li>• 535 km<sup>a</sup> downstream</li> <li>• &lt;1 year<sup>b</sup></li> <li>• 0.09 km<sup>2c</sup></li> <li>• - km GPR</li> <li>• 5 cores</li> </ul>	<ul style="list-style-type: none"> <li>• Low-lying bar exposed at low flow has been in its current location since 2006</li> </ul>	<ul style="list-style-type: none"> <li>• GPR attempted, but radar signal was attenuated</li> </ul>	<ul style="list-style-type: none"> <li>• 5 cores contained 32% ripples and 23% dune sets.</li> <li>• 2 bar-scale sets (20% of core length) were underlain by fine-grained bottomsets that coarsen-upward into its angle-of-repose strata (Fig. 10 E,F)</li> <li>• Trenches revealed bar-scale cross strata with contrast in grain size between 50-60 μm and 190-310 μm (Fig. 10B)</li> </ul>
<p><b>D3</b></p> <ul style="list-style-type: none"> <li>• 537 km<sup>a</sup> downstream</li> <li>• &gt;38 years<sup>b</sup></li> <li>• 1.25 km<sup>2c</sup></li> <li>• - km GPR</li> <li>• no cores</li> </ul>	<ul style="list-style-type: none"> <li>• Sandy bar tail attached to large vegetated island 2 km downstream from D2 and has been in its current location since the earliest satellite images</li> </ul>	<ul style="list-style-type: none"> <li>• GPR attempted, but radar signal was attenuated</li> </ul>	<ul style="list-style-type: none"> <li>• Two trenches revealed medium-scale sets interbedded with co- and return-flow ripple-sets and clay layers with grain sizes of 40, 230, and 280 μm respectively (Fig. 10A)</li> </ul>

<sup>a</sup> relative to the confluence of the Río Paraná and Río Paraguay; <sup>b</sup> approximate age at the time of the survey (2008); <sup>c</sup> Bar area measured at 11400 m<sup>3</sup> s<sup>-1</sup> in December 2008; \* Studied by Sambrook Smith *et al.* (2009)

1  
2  
3  
4  
5  
6  
7  
8  
9  
10  
11  
12  
13  
14  
15  
16  
17  
18  
19  
20  
21  
22  
23  
24  
25  
26  
27  
28  
29  
30  
31  
32  
33  
34  
35  
36  
37  
38  
39  
40  
41  
42  
43  
44  
45  
46  
47  
48  
49

**Table 2.** Classification scheme of GPR facies described in this study (see also Fig. 3)

Facies	GPR facies description	Sedimentary interpretation - structures	Genetic interpretation - bedforms	Examples of GPR lines*	Conceptual sketch of 2D structures
1	A >50% of reflections are steeper than 20° Commonly straight and relatively low amplitude	Large-scale angle-of-repose cross strata with complex pre/re-sorting patterns (see text)	Primarily avalanche deposition at angle-of-repose bar slopes. Could also include some very large dunes		
	B >50% of reflections >6° and <20° Commonly irregular and higher amplitude	Co-sets of inclined small- and medium-scale sets	Primarily dunes and ripples migrating over bar-scale slopes below-the angle-of-repose		
2	>50% of reflections <6° with undular, discontinuous, or chaotic shapes	Near-horizontal small- and medium-scale sets, may include large-scale cross strata with insufficient contrast in properties to generate reflections	Primarily dunes and ripples migrating over near-horizontal surfaces (e.g. channel floor, bar-top)		
3	High-amplitude, laterally-extensive reflections, commonly associated with loss of radar signal	Primarily near-horizontal fine-grained layers of small-scale sets, distinct contrasts in grain size	Large-scale bounding surfaces such as unit-bar bottomsets and low-flow stage deposits, commonly finer-grained, not limited to clay		

\* Images have heights of 2 m and lengths of 20 m

**Table 3.** Percentages of vertical associations of facies calculated from the ~0.1 m spaced vertical profiles.

(a)		Overlying facies			
		1A	1B	2	3
Underlying Facies	1A		2	17	17
	1B	2		17	18
	2	7	18		65
	3	91	80	66	

1  
2  
3  
4  
5  
6  
7  
8  
9  
10  
11  
12  
13  
14  
15  
16  
17  
18  
19  
20  
21  
22  
23  
24  
25  
26  
27  
28  
29  
30  
31  
32  
33  
34  
35  
36  
37  
38  
39  
40  
41  
42  
43  
44  
45  
46  
47  
48  
49  
50  
51  
52  
53  
54  
55  
56  
57  
58  
59  
60

**Table 4:** Percentages silt and clay, sand and gravel, number of samples, and median grain sizes of the investigated bars. Note the downstream increase in clay.

bar	silt/clay%	sand%	gravel%	n	D <sub>50</sub> (μm)
U1	1	99	0	26	263
U2	2	96	2	56	315
U3	0	99	1	16	361
U5	9	90	1	27	348
C1	31	69	0	13	141
C2	11	89	0	26	244
D1	13	87	0	37	237
D2	12	88	0	25	251
D3	23	77	0	3	181

1  
2  
3  
4  
5  
6  
7  
8  
9  
10  
11  
12  
13  
14  
15  
16  
17  
18  
19  
20  
21  
22  
23  
24  
25  
26  
27  
28  
29  
30  
31  
32  
33  
34  
35  
36  
37  
38  
39  
40  
41  
42  
43  
44  
45  
46  
47  
48  
49  
50  
51  
52  
53  
54  
55  
56  
57  
58  
59  
60

Draft paper: Variability in bar sedimentology in a large river, Version 6, 09/03/2011

**Table 5:** Core lengths and percentages of sedimentary structures in the cores.

Cores	core length	ripples	dunes	bars	low-stage plane bed	upper-stage plane bed	unknown or deformed
all	152.95	35	26	16	1	0	22
upstream	95.37	31	27	20	0	0	22
downstream	57.58	43	24	8	2	0	24
U1	51.09	43	11	22	0	0	23
U2	35.33	19	51	12	0	0	18
U3	4.99	2	26	72	0	0	0
U5	3.96	16	21	0	0	3	60
C1	4.20	36	25	0	8	0	30
C2	13.01	15	15	4	1	0	24
D1	19.93	46	32	0	2	0	20
D2	20.44	32	23	20	1	0	25